VERIFICATION

UDM CHAPTER 5: TRANSITIONS

DATE: December 2023

No.	Date	Reason for Issue	Prepared by	Verified by	Approved by
1	1999	PHAST 6.0	Witlox and Holt		
2	May 2011	Phast 6.7; v2 UDM	Harper		
3	May 2021	Apply new template	D. Vatier		

Date: December 2023

Prepared by: Digital Solutions at DNV

ABSTRACT

The transitions in the UDM have been studied in detail.

Plume touchdown
The original UDM 5.2 method for dissipating vertical momentum during touchdown was incorrect. This lead to erroneous excessive acceleration of the cloud in the downwind direction. In addition it involved an arbitrary 'plume impact parameter' for conversion of vertical into horizontal momentum.

A new plume impact formulation has been included, which applies a plume impact force perpendicular to the plume axis during touchdown (assumption of elastic collision). A sensitivity analysis has been carried out to investigate the new formulation for both cases of continuous and instantaneous dispersion.

Passive transition
The UDM theory for transition to passive and inclusion of averaging times has been investigated in detail. Several modifications to the UDM 5.2 code have been applied:

1. The UDM 5.11 passive-transition criterion [cloud density close to ambient density] has been refined:
   a. The cloud velocity must be close to the ambient velocity to avoid transitions for high-speed jets
   b. The passive type of entrainment must be close to the total entrainment to avoid transition if non-passive entrainment is still significantly large
   c. The Richardson number must be sufficiently small for a heavy-gas grounded plume, to avoid transition if the heavy entrainment is significantly different from passive entrainment

2. The UDM 5.2 averaging-time treatment overestimated the averaging-time effect along the transition distance. For averaging time t_{av} larger than the core averaging time t_{av}^{core} this leads to too high width and too low maximum concentration, while for $t_{av} < t_{av}^{core}$ the opposite occurs (even up to the extent of reduction of cloud width and increase of concentration). The UDM 5.2 method is retained as the default option within the current UDM using the fixed core averaging time t_{av}^{core}=18.75 s.

   To avoid the above, an option has been implemented into the current UDM to allow a variable core averaging time, such that t_{av} can be chosen equal to t_{av}^{core}. This leads to a much smoother transition. This method is, however, more CPU-intensive for a range of user-specified averaging times.

3. Far-field passive spread in now also phased in (consistent with the phasing in of passive entrainment), which leads to smoother transitions.

Table of contents

5 UDM TRANSITIONS

5.1 Touchdown (plume impact)

This section examines the new formulation for the plume impact force exerted by the ground during touchdown. Both cases of continuous and instantaneous dispersion are considered.

5.1.1 Continuous dispersion

In this section a sensitivity analysis is carried out to investigate the new plume impact formulation for continuous dispersion. The base case is selected as follows:

- horizontal 2-phase propane release (80% liquid)
- release rate 70 kg/s
- release velocity 20 m/s
- release height 3 m
- droplet size 0.0001 m
- non-equilibrium, no rainout
- stability class D1.5

Three types of parameter variations for the above base case have been carried out:

1. Figure 5.1 includes results for variation of the ambient wind speed (u_a = 1.5, 5, 10 or 25 m/s). The point of impact is further downwind for increasing wind speed (Figure 5.1a). As described in the theory manual, the plume impact force is present during touching down, and points perpendicular to the plume axis (in the downwind direction). This results in a extra deflection of the plume axis in the downwind direction during touching down. After touching down, the plume axis is horizontal (at ground level).

2. Figure 5.2 includes results for variation of the release angle (ϕ_R = 0°,30°, 60°, 90°, -60°). For ϕ_R = 60°, 90°, -60°, the incident angle to the ground is very high (Figure 5.2a). The large vertical component of the cloud centre-line velocity is reset to zero after touching down, which results in a discontinuity to the centre-line velocity (Figure 5.2b). This behaviour of the cloud for the large impact angles seems to be conceptually correct i.e. the cloud velocity decreases rapidly at touchdown and the cloud rapidly spreads (see Figure 5.2c).

   Note that the model does not take into account the effect of entrainment resulting from additional turbulence generated by a jet impinging on the ground. Therefore the model may be less accurate if the incident angle and/or impact speed are large.

3. Figure 5.3 includes results for variation of the release velocity (1, 20 or 100 m/s). For the 1 m/s release velocity, the large incident angle results in a discontinuity in the centre-line velocity for reasons as discussed above.

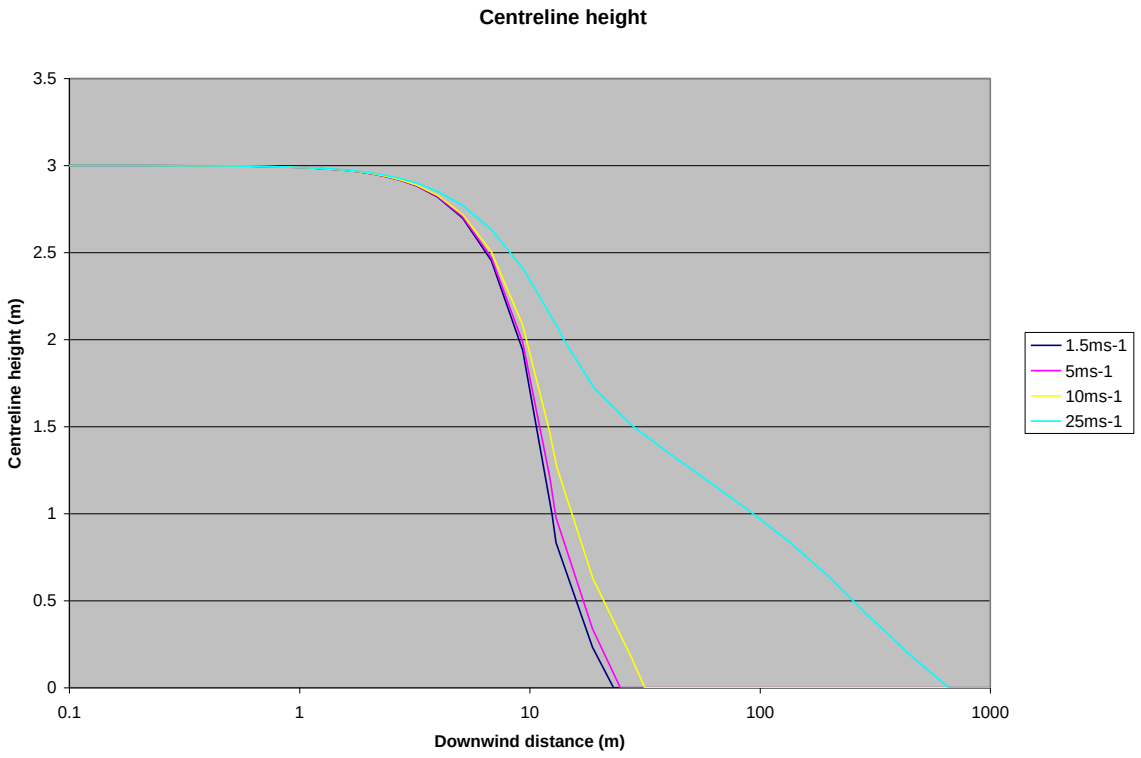

(a) centre-line height

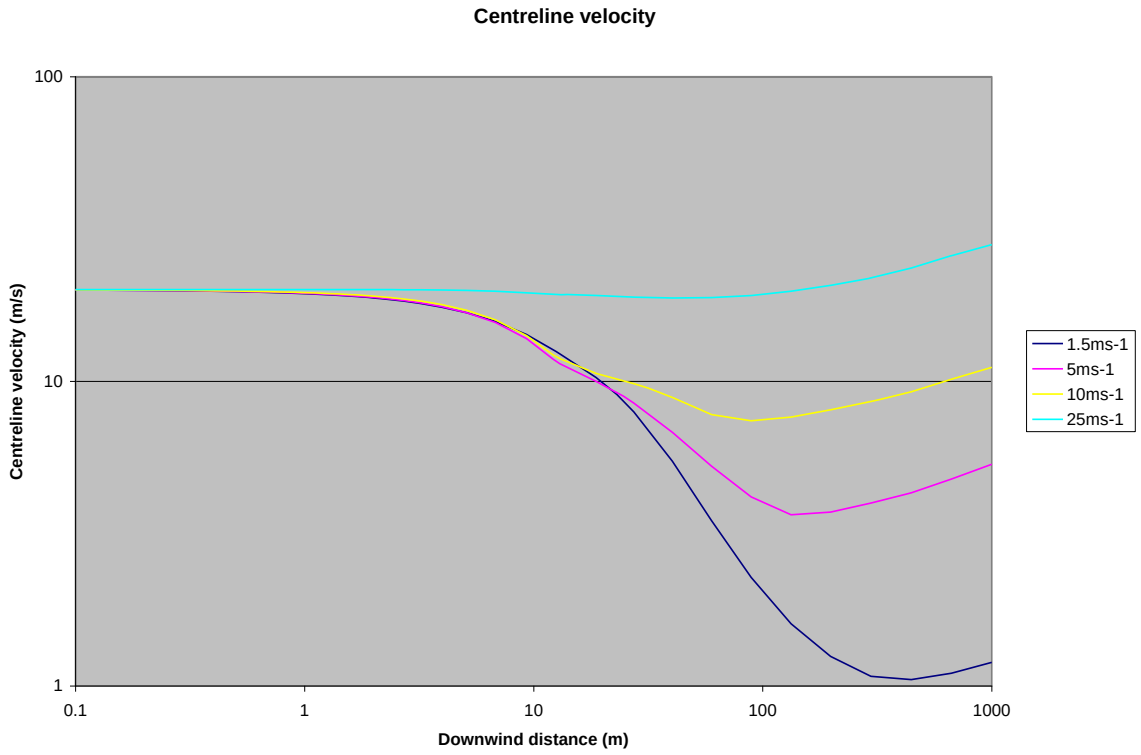

(b) centre-line velocity

Figure 5.1 Elevated two-phase propane release; variation of ambient wind speed (u_a = 1.5, 5, 10, or 25 m/s)

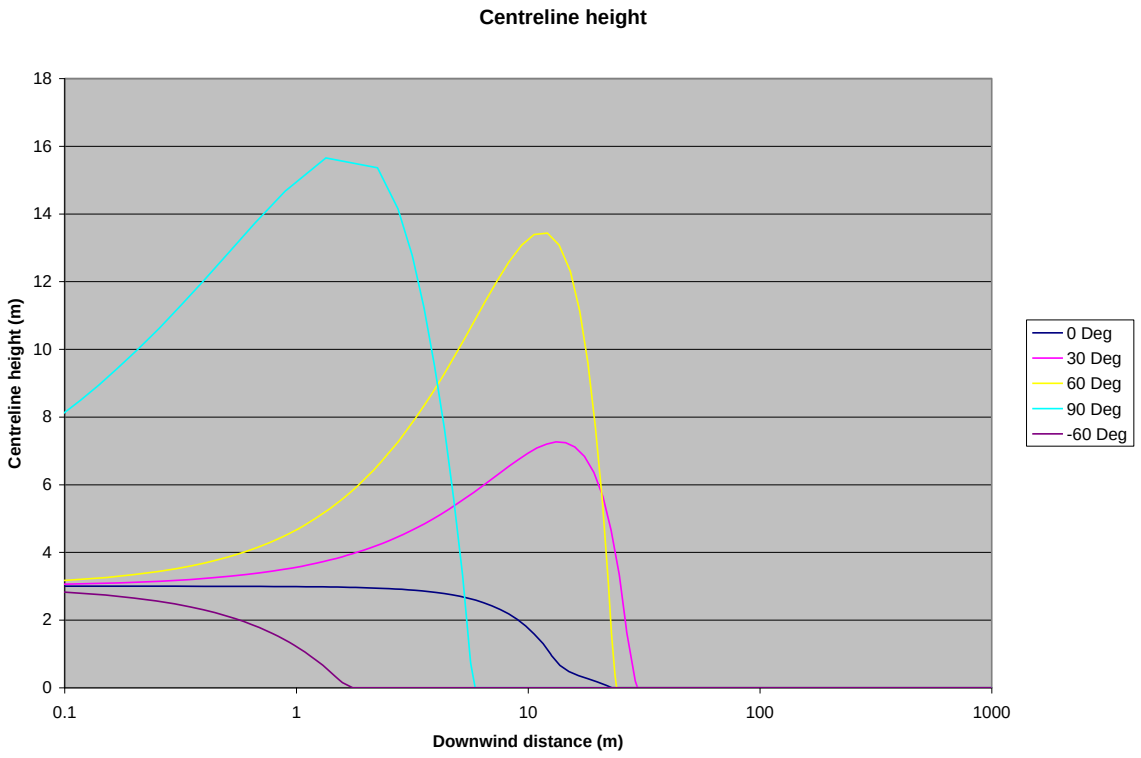

(a) centre-line height

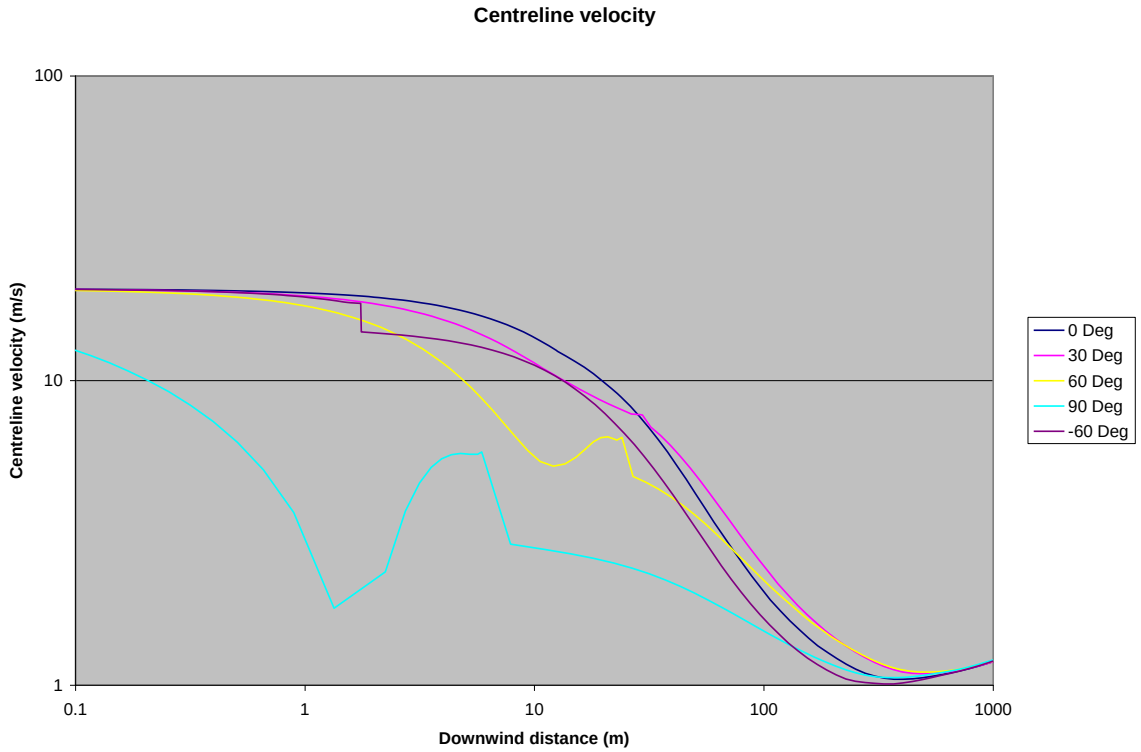

(b) centre-line velocity

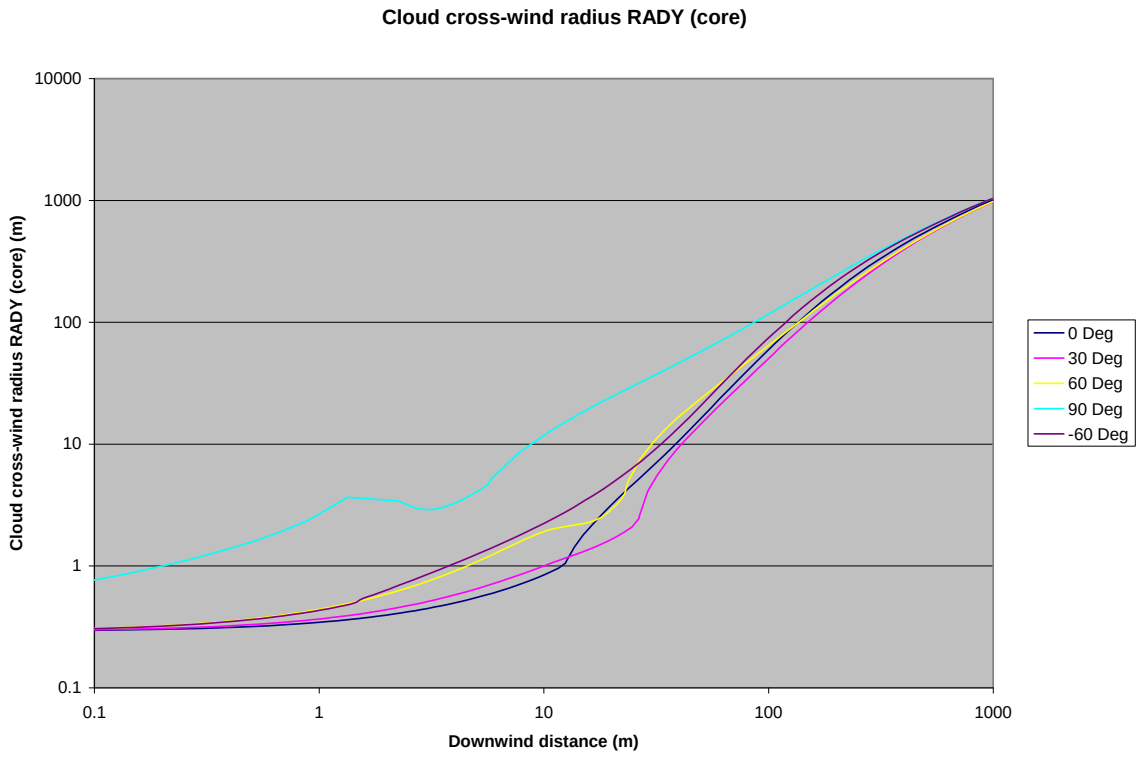

(c) cloud half-width R_y

Figure 5.2 Elevated two-phase propane release; variation of release angle (ϕ_R = 0º, 30º, 60º, 90º, -60º)

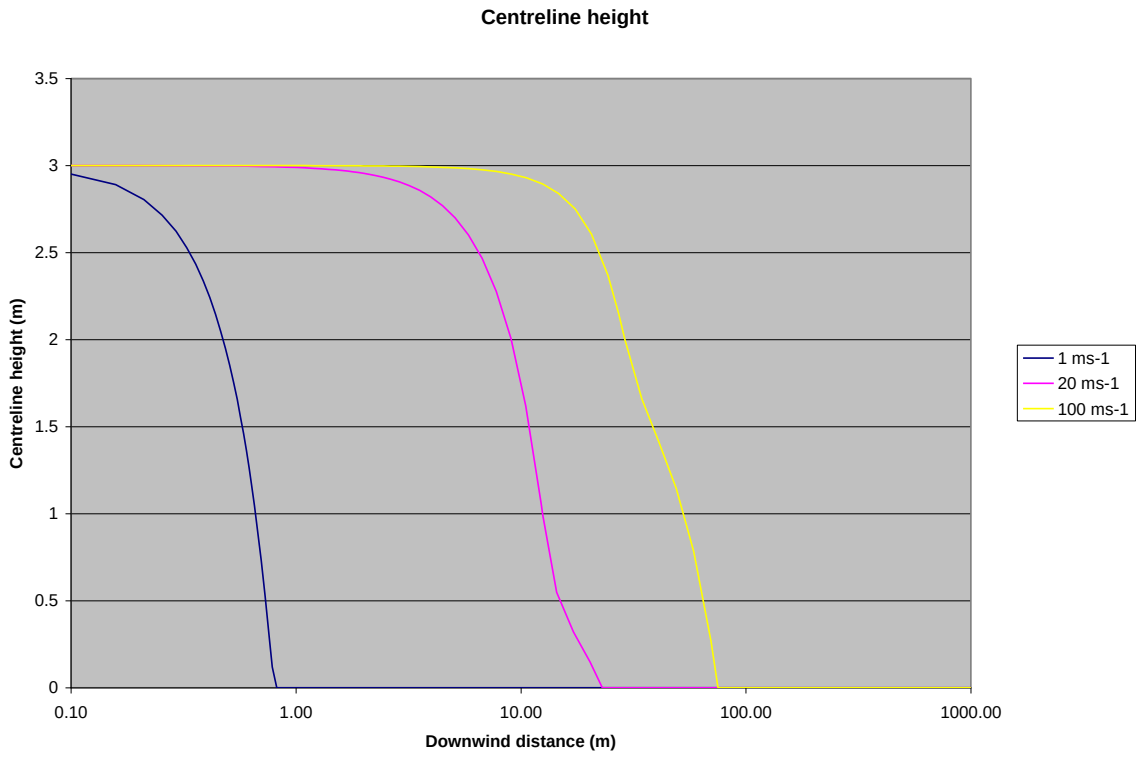

(a) centre-line height

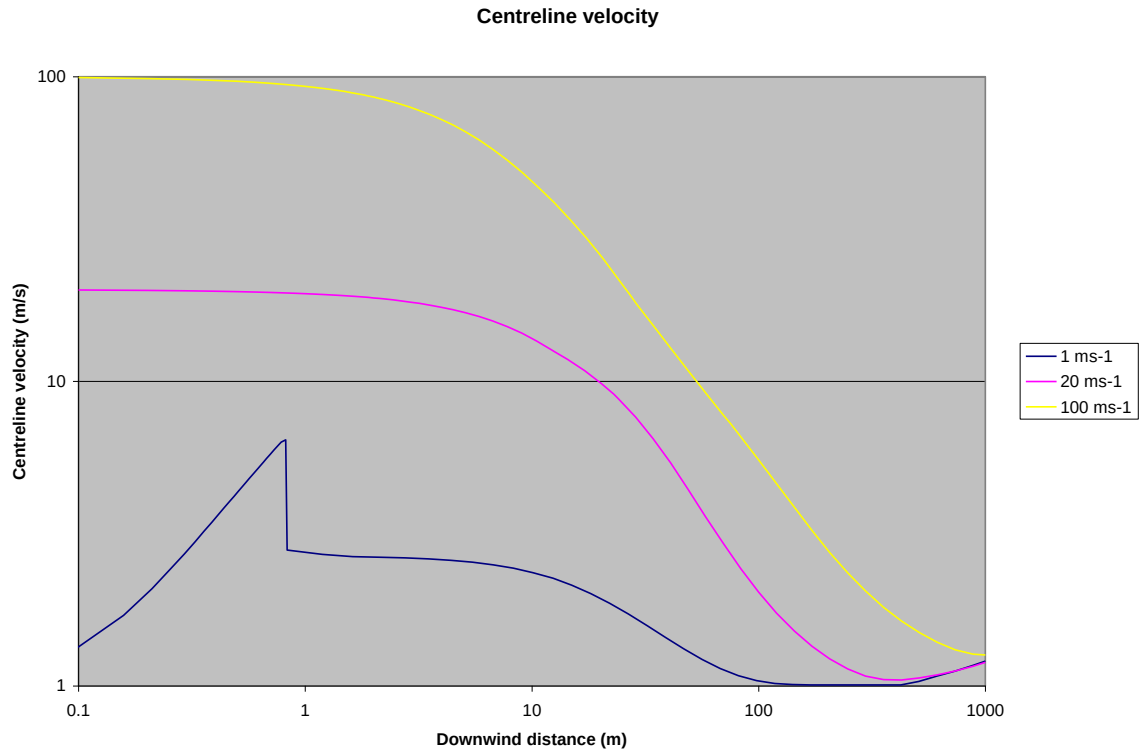

(b) centre-line velocity

Figure 5.3 Elevated continuous two-phase propane release; variation of release speed (1, 20, or 100 m/s)

5.1.2 Instantaneous dispersion

In this section a sensitivity analysis is carried out to investigate the new plume impact formulation for instantaneous dispersion. The base case is selected as follows:

- horizontal 2-phase propane release (80% liquid)
- release rate 1000 kg (release velocity 0.01 m/s)
- release height 3 m
- droplet size 0.0001 m
- non-equilibrium, no rainout
- stability class D1.5

A parameter variation was carried out to the ambient wind speed (1.5, 5, 10 or 25 m/s). From the results shown in Figure 5.4, the following conclusions are drawn for the lower wind speeds of 1.5 and 5 m/s:

- At cloud impact the cloud velocity rapidly decreases.
- Immediately following cloud impact the entrainment rate is very large leading to an increase in centroid height, which results in an increase of cloud velocity.
- As the cloud slumps the ambient velocity at the centroid height rapidly decreases leading to a reduction in the cloud velocity.
- In the far-field, passive ambient turbulence/spreading takes over from gravitational slumping leading to an increase of centroid height, and therefore an increase in cloud velocity.

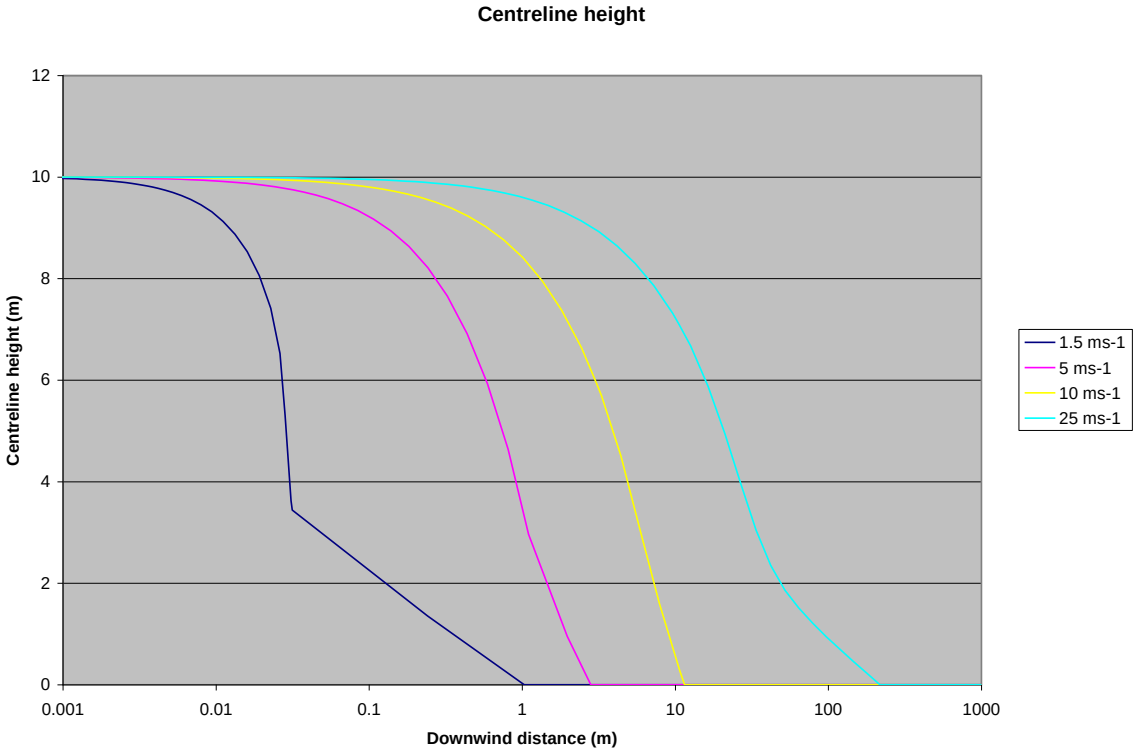

(a) centre-line height

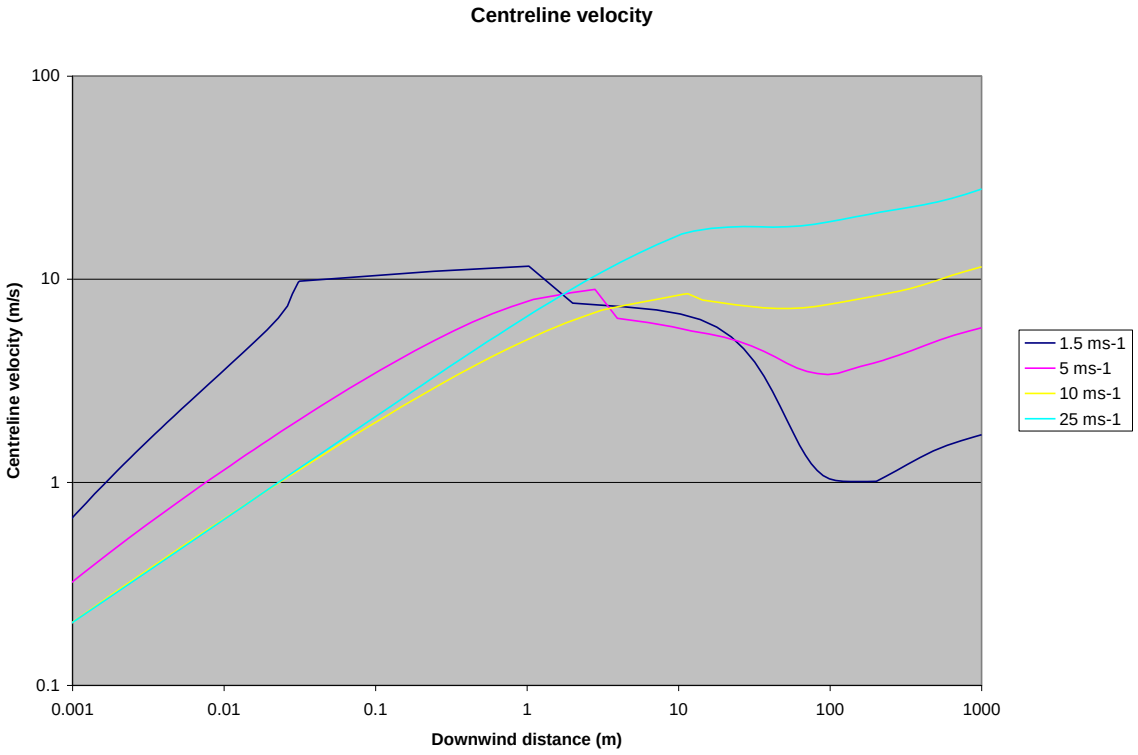

(b) centre-line velocity

Figure 5.4 **Elevated instantaneous two-phase propane release; variation of ambient wind speed (u_a = 1.5, 5, 10, or 25 m/s)**

5.2 Passive transition

This section reports the verification of the logic for phasing in of passive spread, entrainment and averaging time along the transition zone. As stated in the UDM theory manual the current formulation is as follows.

5.2.1 Phasing in of passive spread/entrainment

The transition distance x_{tr}^{pas} is the downwind distance at the onset of transition to passive, and $r_{tr}x_{tr}^{pas}$ the end of transition to passive. Along the transition zone $x_{tr}^{pas} < x < r_{tr}^{pas}\, x_{tr}^{pas}$, the near-field entrainment E_{tot}^{nf} and spread rate $(dR_y/ds)^{nf}$ are phased out, while the far-field passive entrainment E_{pas}^{ff} and passive spread rate $(dR_y/ds)^{ff} = d\sigma_{ya}/dx$ are phased in:

$$\begin{aligned} dR_y/ds &= [1-f(x)]\ (dR_y/ds)_{nf} + [f(x)]\ 2^{1/2}(d\sigma_{ya}/ds) \\ E_{tot} &= [1-f(x)]\ E_{tot}^{nf} + [f(x)]\ E_{pas}^{ff} \end{aligned} \qquad \textbf{(5.1)}$$

where the linear smoothing function f(x) is given by $f(x) = [x - x_{tr}^{pas}]/[\, r_{tr}^{pas}\, x_{tr}^{pas} - x_{tr}^{pas}]$. The above transition is needed to avoid discontinuous entrainment and discontinuous spread rate. This willsmoothen curves, but retains the disadvantage of a rather arbitrary transition distance.

5.1.1 Methods for phasing in passive dispersion and averaging-time effect

The ambient cross-wind dispersion coefficient at the averaging time t_{av} is obtained from that at the core averaging time of t_{av}^{core} by

$$\sigma_{ya}(t_{av}) = \sigma_{ya}(t_{av}^{core})\left(\frac{t_{av}}{t_{av}^{core}}\right)^{0.2} \qquad \textbf{(5.2)}$$

Listed below are a number of potential UDM methods for phasing in passive dispersion and averaging time effects. Note that methods A and B are currently implemented; method A is the recommended method, although method B is less CPU time-intensive.

A. <u>UDM analysis with averaging time equal to core averaging time: $t_{av}^{core} = t_{av}$</u>

In this case the averaging time effect is already included in the core $\sigma_{ya}^{core} = \sigma_{ya}$, and averaging-time effects will automatically be phased in along the transition zone as part of the phasing in of passive spread. Thus the post-processor RPRO does not need to do any additional time averaging, i.e. the values for the cross-wind dispersion coefficient σ_y and maximum concentration c_o equal the core values:

$$\sigma_y = \sigma_y^{core}, \quad c_o = c_0^{core} \qquad for\ t_{av} = t_{av}^{core} \qquad \textbf{(5.3)}$$

B. <u>UDM analysis with averaging time different to core averaging time: $t_{av}^{core} \neq t_{av}$</u>

Less accurate predictions will now be obtained. However it will be less CPU-intensive if calculations for a range of averaging times is desired. RPRO now needs to apply the averaging-time correction $r_{avcor} = (t_{av}/t_{av}^{core})^{0.2}$ [phased in along the passive transition zone]:

$$\begin{aligned} &\sigma_y = \sigma_y^{core}, \quad c_o = c_0^{core} && for\ x < x_{tr}^{pas} \\ &\sigma_y = \{[1-f(x)] + f(x)\, r_{avcor}\}\sigma_y^{core}, \ c_o = \{[1-f(x)] + f(x)\, r_{avcor}\}c_o^{core} && for\ x_{tr}^{pas} < x < r_{tr}^{pas}x_{tr}^{pas} \\ &\sigma_y = r_{avcor}\sigma_y^{core}, \ c_o = r_{avcor}c_o^{core} && for\ x > r_{tr}^{pas}x_{tr}^{pas} \end{aligned} \qquad \textbf{(5.4)}$$

This method is not consistent with the approach adopted in the UDM core calculations and over-estimates the effect of averaging-time along the transition zone. For $t_{av} < t_{av}^{core}$ this leads to too much averaging-time phasing-down of cloud width σ_y and too much phasing up of the centre-line concentration c_o. For $t_{av} > t_{av}^{core}$ it leads to too much phasing-up of σ_y and too much phasing-down of c_o.

C. UDM analysis with $t_{av}^{core} \neq t_{av}$ and improved averaging-time treatment for σ_y (and??)

This overcomes the problem for Method B for phasing in of averaging time for cloud width. However improved calculation of the resulting centre-line concentration needs to be further investigated.

$$\begin{aligned}
&\sigma_y = \sigma_y^{core}, \quad c_o = c_0^{core} && for\ x < x_{tr}^{pas} \\
&\sigma_y = \sigma_y(x_{tr}^{pas}) + [\sigma_y^{core}(x) - \sigma_y(x_{tr}^{pas})]\{1 - f(x)] + f(x)\, r_{avcor}\}, \ c_o = ??? && for\ x_{tr}^{pas} < x < r_{tr}^{pas} x_{tr}^{pas} \\
&\sigma_y = \sigma_y(x_{tr}^{pas}) + [\sigma_y^{core}(x) - \sigma_y(x_{tr}^{pas})] r_{avcor}, \quad c_o = ??? && for\ x > r_{tr}^{pas} x_{tr}^{pas}
\end{aligned}$$

(5.5)

D. UDM analysis with virtual sources such that R_y, R_z are continuous

1. Set virtual-source distance x_{vy} from solving $R_y(x_{tr}^{pas})=2^{1/2}\ \sigma_{ya}(x_{tr}^{pas} - x_{vy}; t_{av}=18.75)$. Note that the instantaneous value of the averaging time is used in the above matching criterion.
2. Set virtual-source distance x_{vz}
   * For a ground plume, set x_{vz} from solving $R_z(x_{tr}^{pas})=2^{1/2}\ \sigma_{za}(x_{tr}^{pas} - x_{vz})$
   * For an elevated plume, an analogous procedure cannot be done since the UDM does not adopt the (TNO) passive dispersion profile [see passive-dispersion sensitivity analysis; h_d effect]. Instead the concentration profiles may be matched in some kind of way, to yield some equation for $\sigma_{za}(x_{tr}^{pas} - x_{vz})$ from which x_{vz} could be set.
3. In post-processor RPRO (applicable for $t_{av} \neq t_{av}^{core}$ only) :
   * For $x < x_{tr}^{pas}$, apply no time averaging
   * For $x > x_{tr}^{pas}$, set $\sigma_y(x;t_{av}) = \sigma_y(x_{tr}^{pas}) + [\sigma_y^{core}(x) - \sigma_y(x_{tr}^{pas})][t_{av}/t_{av}^{core}]^{0.2}$
     set concentration using the above modified $\sigma_y(x;t_{av})$, and applying reduced maximum concentration (how??)

The above type of approach is more commonly adopted, e.g. in TNO and HGSYSTEM dispersion models. The disadvantage is that concentration slopes, $dR_y dx$, dR_z/dx may be discontinuous, but it is not considered less accurate! The advantage is there is no arbitrary transition distance.

E. UDM analysis such that dR_y/dx, dR_z/dx are continuous ($r_{trpas}=1$)
This will implicitly also imply continuous entrainment rate (for instantaneous averaging time), and therefore concentration slopes. The disadvantage is that appropriate virtual sources may not be found, or are unphysical. Also the approach is different to that normally adopted.

F. UDM analysis with transition point such that continuous entrainment
Remove transition distance. At every downwind distance, calculate virtual sources such that R_y, R_z are continuous and set E_{pas}^{ff}. Apply transition point at point for which $E_{tot} = E_{pas}^{ff}$ and other transition criteria satisfied. This is an unusual approach. Note that for comparison reasons E_{pas}^{ff} should be based on 18.75 seconds since wind meander does not have effect for the initial jet (or ditto heavy plume). Time averaging to be applied after the transition only to make life easy! Virtual source values x_{y0} and x_{zo}, such that instantaneous values are continuous for σ_{ya} and σ_{za}. At the passive transition the entrainment slope is continuous for the instantaneous averaging time only.

5.1.2 Comparison of UDM results between methods

To verify the above method and compare them with the former UDM5.2 method, simulations have been carried out for the following three types of scenarios:

- Passive transition for elevated air jet (no touching down; release height 500 m)

  The input data correspond to the base-case problem for jet dispersion (see Chapter 3 of the UDM verification report).

- Passive transition for elevated air jet (during touching down; release height 5 m)

  The input data are as above, but with reduced release height.

- Transition to passive for ground-level heavy plume (propane)

This heavy-gas case corresponds to the steady ground-level release of 10 kg/s propane with a release velocity of 5 m/s. Isothermal conditions apply (temperature of 298 K) with stability class D5, uniform ambient profiles and roughness length z_o = 0.1m.

To study the effect of averaging time, calculations are carried out for averaging times t_{av} = 18.75 (instantaneous), 60, 600 and 3600 seconds.

The above simulations have been carried out using different types of model assumptions for the phasing in of the spread rate and the treatment of averaging-time effects:

Old UDM method [10 minutes core-averaging time]
t_{av}^{core} = 600 s; no phasing in of spread rate; old UDM averaging-time method B
[see Figure 5.5, Figure 5.6 and Figure 5.7]

Using the core-averaging time t_{av}^{core} = 600 s larger than the instantaneous value t_{av}^{ins} = 18.75 s, leads to the possibility of the averaging time less than the core-averaging time. For t_{av} = 18.75 s the correction equals $(t_{av}/t_{av}^{core})^{0.2}$ = 0.5. Thus downwind of the passive-transition zone the averaging-time correction Method B [Equation (5.4)] leads to halving the width and doubling the maximum concentration. This results in the following:

- For the heavy-gas case, the cloud half-width reduces at the start of the passive-transition zone. This is clearly wrong and caused by the too coarse method B (Figure 5.5b)].

- For the touchdown-jet case, the centre-line concentration increase (Figure 5.7a)

For the elevated-jet case, the cloud depth decreases at the point of transition for jet and touching down jet cases. This is due to the instant application of the much larger passive spread rate whilst the entrainment rate is gradually phased in (Figure 5.6c).

Old UDM method [instantaneous core-averaging time]
t_{av}^{core} = 18.75 s; no phasing in of spread rate; old UDM averaging-time method B
[see Figure 5.8, Figure 5.9 and Figure 5.10]

Using the instantaneous core-averaging time t_{av}^{core} = 18.75 leads to the RPRO averaging time always to be larger ($t_{av} > t_{av}^{core}$). As a result the averaging-time correction always leads to increased widths and reduced concentrations. This removes all of the above anomalies, however, there are still severe discontinuities in cloud widths and concentrations at the transition point for $t_{av} > t_{av}^{core}$.

Note that the results are considered equally inaccurate as indicated above for t_{av}^{core}. However these inaccuracies are not so evident for this case and the results look more realistic (but are **not** more realistic).

Improved averaging-time correction for cloud width
t_{av}^{core} = 18.75; no phasing in of spread rate; averaging-time method C (improved width) [see Figure 5.11, Figure 5.12 and Figure 5.13]

As a result of the above shortcomings, averaging-time method C is applied instead of Method B. This improves the averaging-time correction to the width by not applying the averaging-time correction to the entire width, but only to its incremental increase after the onset of passive transition. As a result, cloud widths will never decrease during an averaging-time correction, even not for $t_{av}^{core} > t_{av}$.

As expected, application of Method C instead of Method B reduces the severity of the discontinuity in the cloud width predictions. Since the concentration calculation is not changed, the discontinuities in the centre-line concentration remain.

Variable core-averaging time = actual averaging time (no averaging-time correction)
$t_{av}^{core} = t_{av}$; no phasing in of spread rate; no averaging-time correction - method A
[see Figure 5.14, Figure 5.15 and Figure 5.16]

This method avoids any complications with respect to phasing-in of averaging time. The following is concluded from the figures:

- The discontinuities in the centre-line concentration at the transition point are much less severe, because of removal of need for averaging-time correction.

- The discontinuity in the cloud width predictions become sharper than when compared with the same case in which the averaging time correction is smoothed in (method C). This is caused by the instantaneous application of the passive spread rate.

- For larger averaging times the cloud depth decreases at the point of transition due to the instantaneous application of the passive spread rate.

Variable core-averaging time = actual averaging time, and phasing in of passive spread
$t_{av}^{core} = t_{av}$; phase in spread rate; no averaging-time correction - method A
[see Figure 5.17, Figure 5.18 and Figure 5.19]

This method eliminates the above problems associated with the instantaneous application of passive spread rate. The UDM is now adjusted so that the spread rate is smoothed in over the transition distances. This ensures that the discontinuities at the transition point are much less severe.

This approach is the recommended method for the current UDM.

Old UDM method [instantaneous averaging time, but include phasing in of passive spread]
$t_{av}^{core} = 18.75$; phase in spread rate; old UDM averaging-time method B
[see Figure 5.20, Figure 5.21 and Figure 5.22]

The above recommended method has the disadvantage that separate UDM calculations need to be carried out for each different averaging time. As a result an additional method has been retained, for which the core-averaging time is fixed for a series of averaging times. The passive spread rate is phased in, but the method retains the old UDM averaging-time method B and the problems associated with this.

As can be seen from the figures the discontinuities for the large averaging times are still present. The results are worse than when smoothing in the averaging time correction, however this enhancement has been delayed until a more sophisticated way of applying the average time correction to the centre-line concentration has been found.

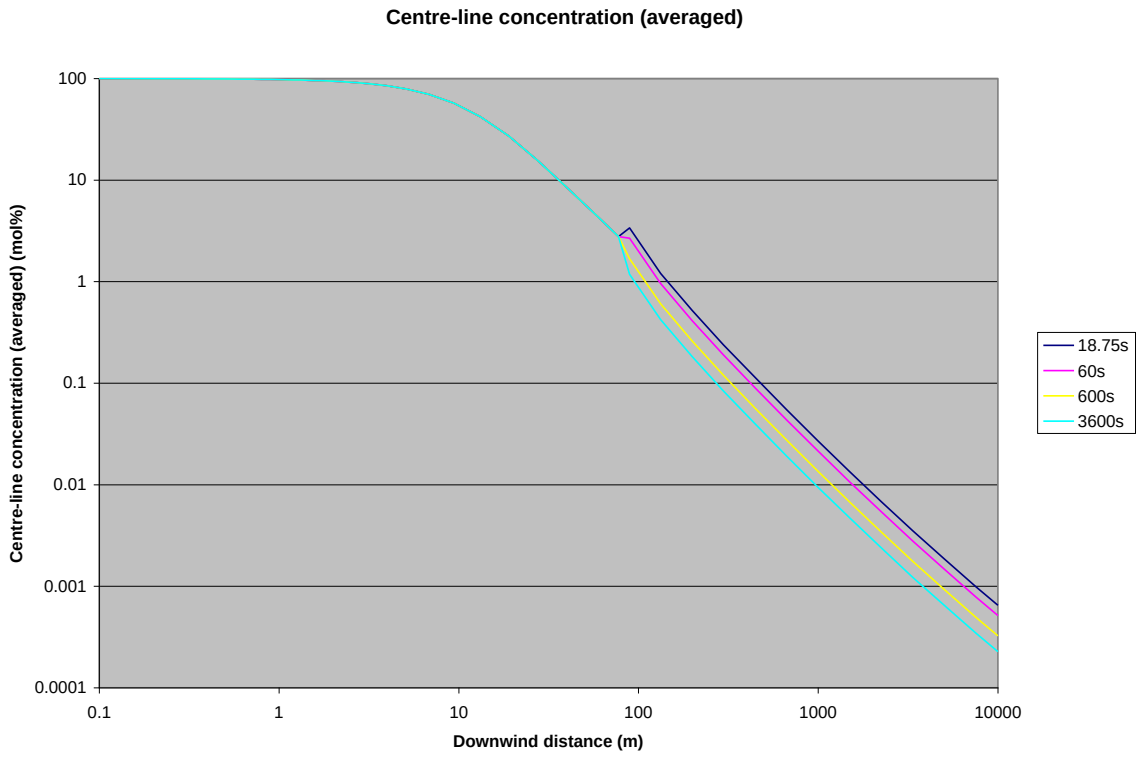

(a) centre-line concentration

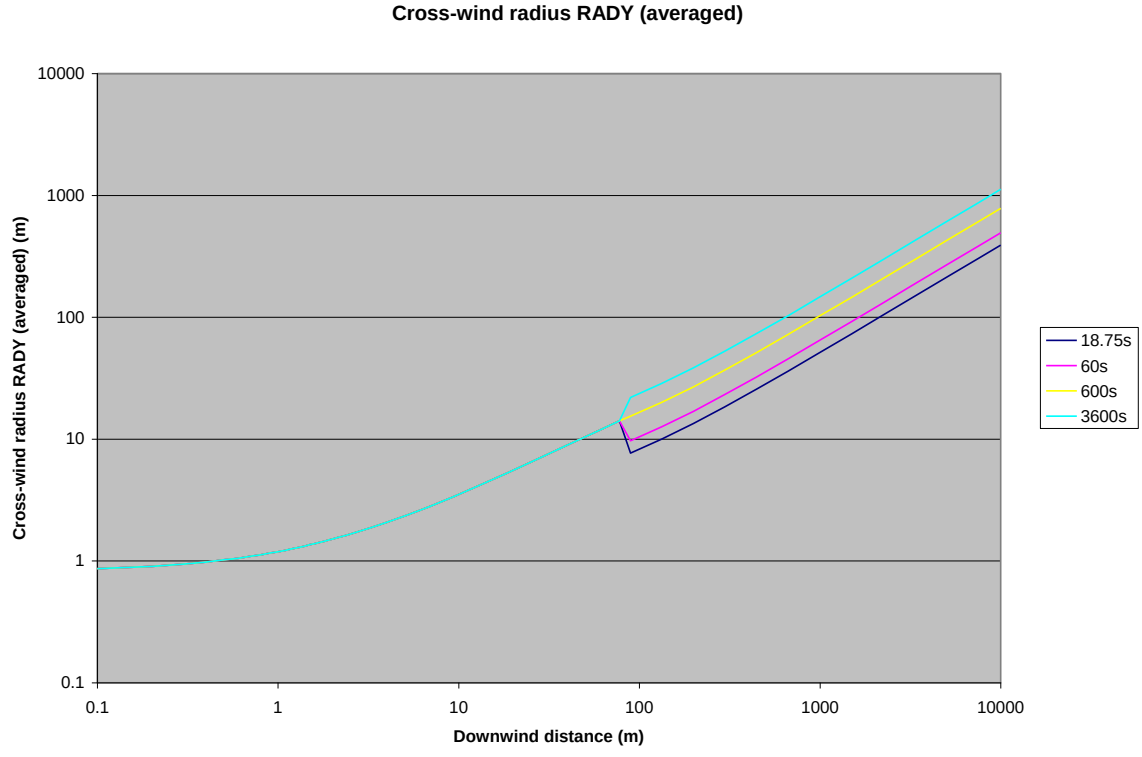

(b) cloud half-width R_y

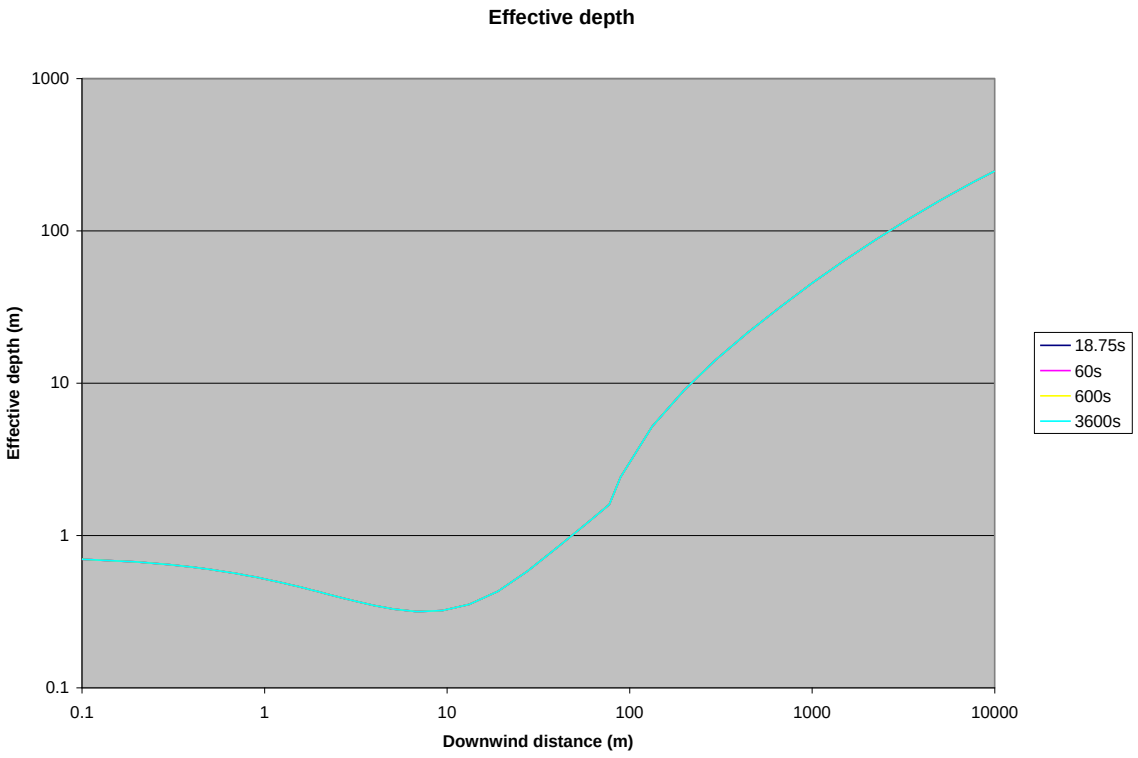

(c) effective depth $H_{eff}(1+h_d)$

Figure 5.5 **Variation of averaging time for heavy-gas base case**
[t_{av}^{core} = 600s; no phasing in of spread rate; averaging-time method B (old UDM)]
UDM predictions are included for averaging times t_{av} = 18.75, 60, 600, 3600 seconds.

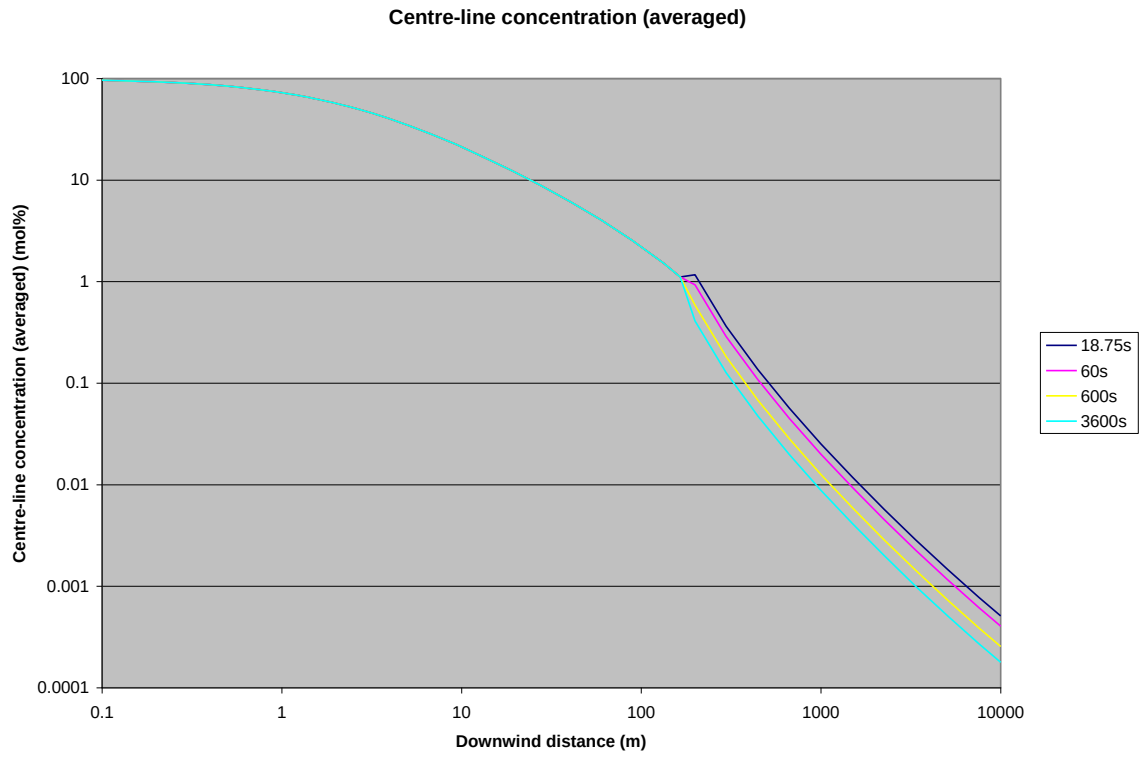

(a) centre-line concentration

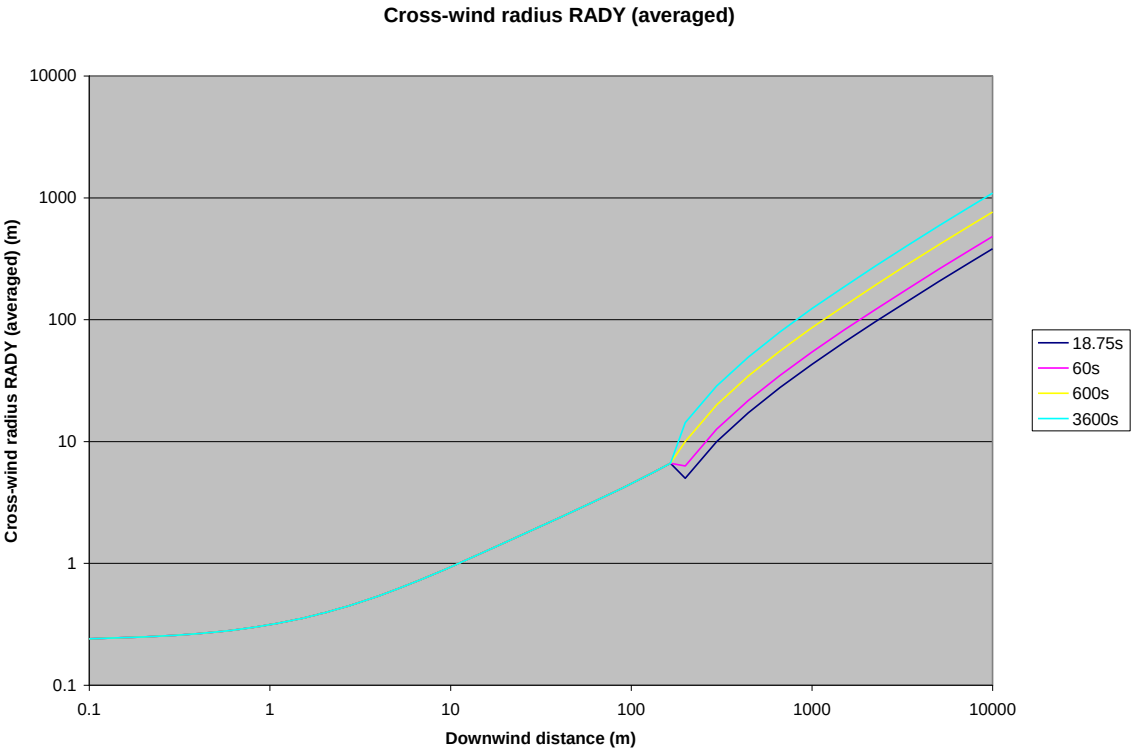

(b) cloud half-width R_y

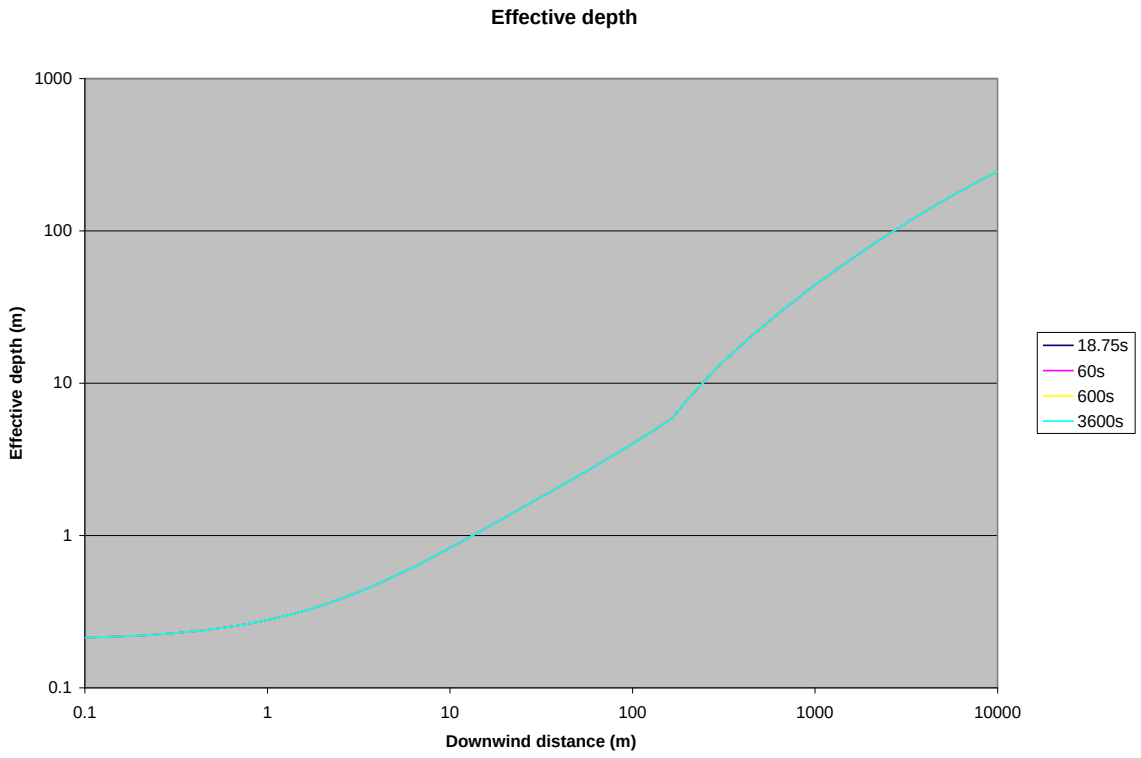

(c) effective depth $H_{eff}(1+h_d)$

Figure 5.6 **Variation of averaging time for elevated-jet base case**
[t_{av}^{core} = 600s; no phasing in of spread rate; averaging-time method B (old UDM)]
UDM predictions are included for averaging times t_{av} = 18.75, 60, 600, 3600 seconds.

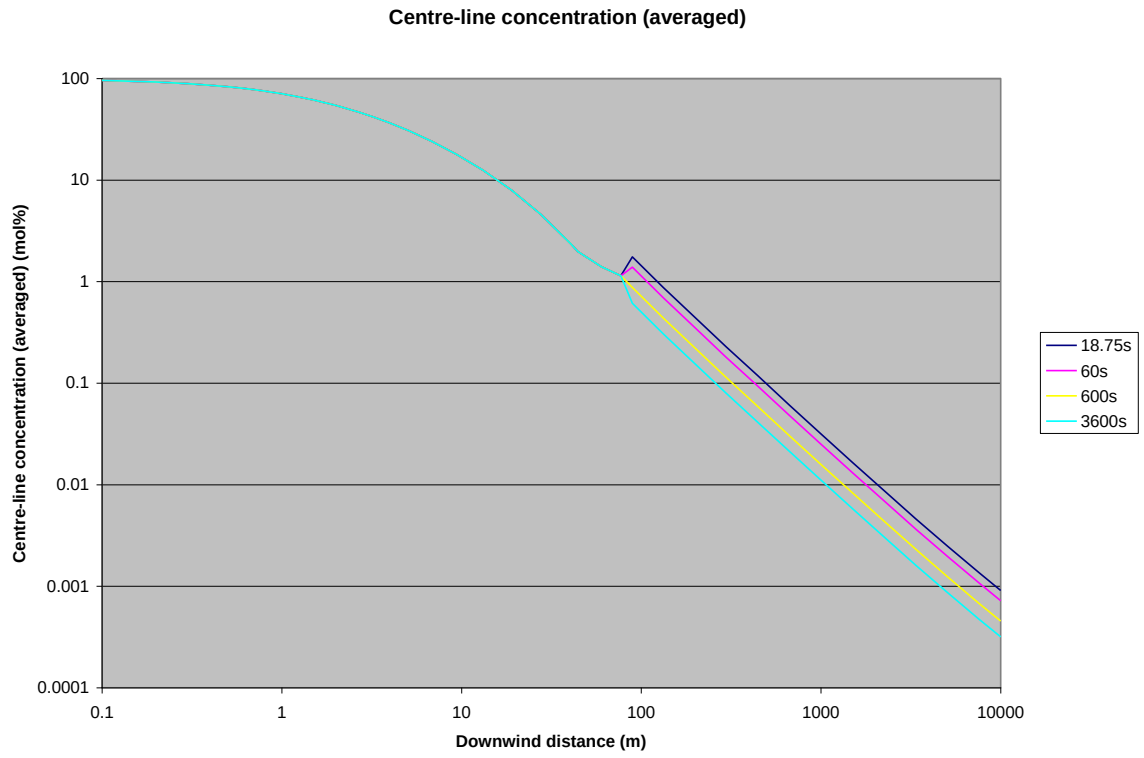

(a) centre-line concentration

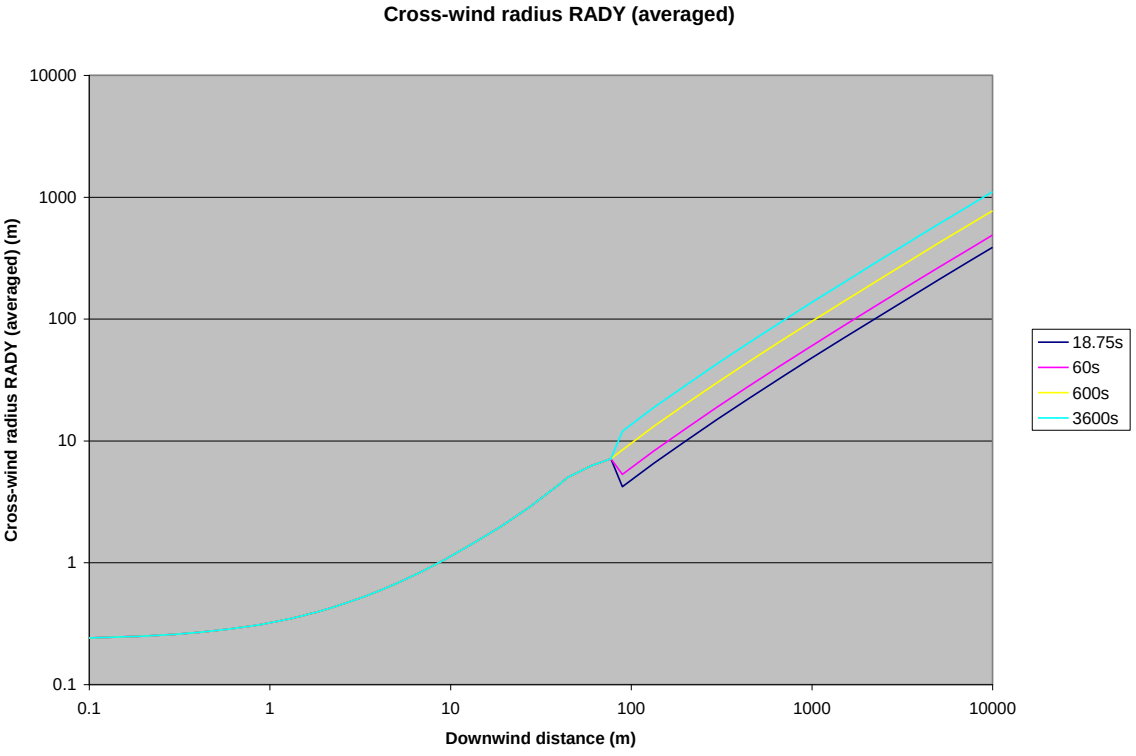

(b) cloud half-width R_y

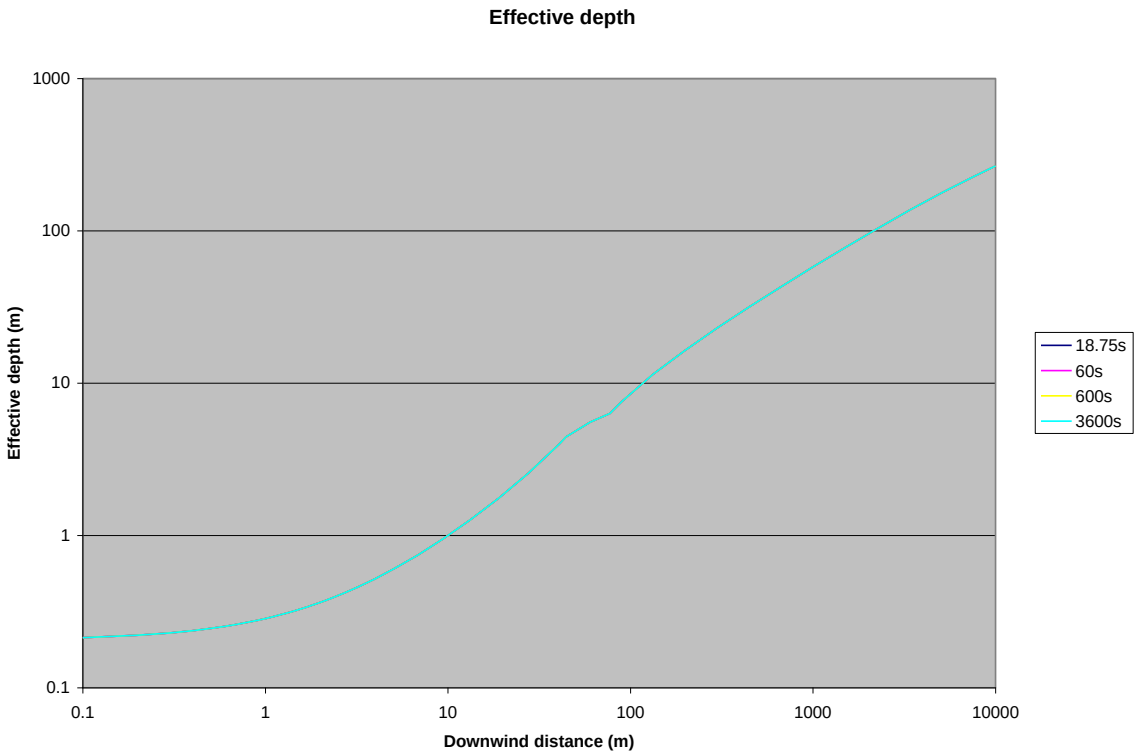

(c) effective depth $H_{eff}(1+h_d)$

Figure 5.7 **Variation of averaging time for touching-down jet base case**
[t_{av}^{core} = 600s; no phasing in of spread rate; averaging-time method B (old UDM)]
UDM predictions are included for averaging times t_{av} = 18.75, 60, 600, 3600 seconds.

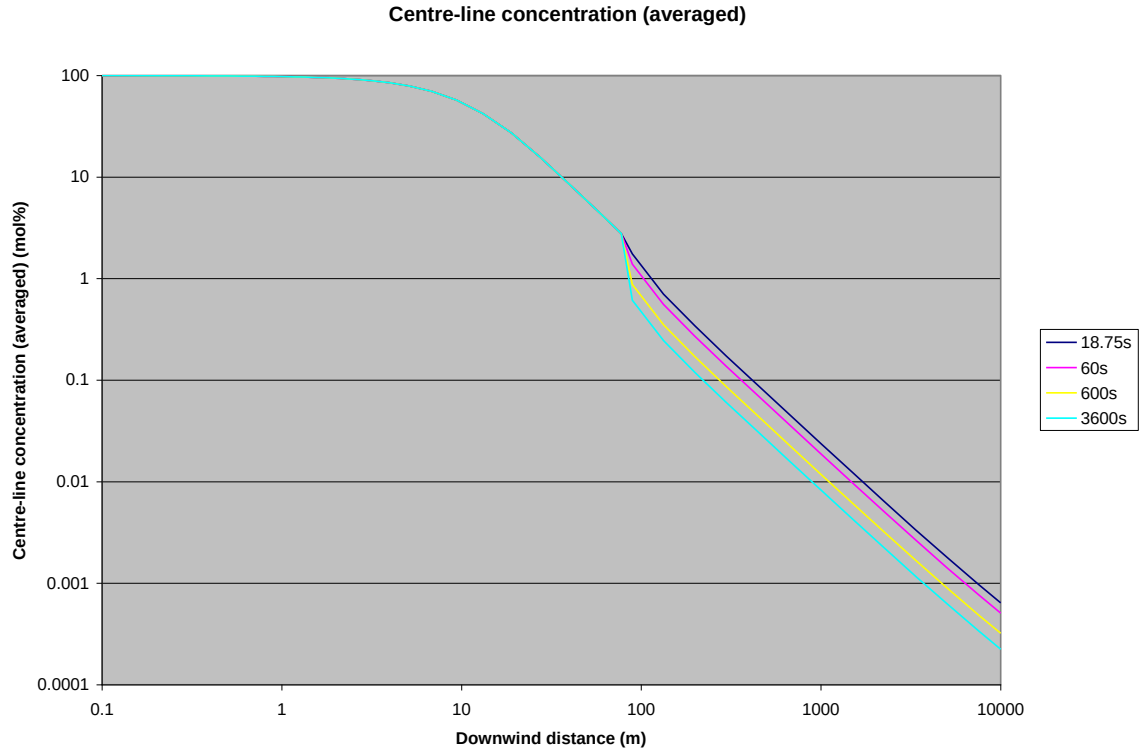

(a) centre-line concentration

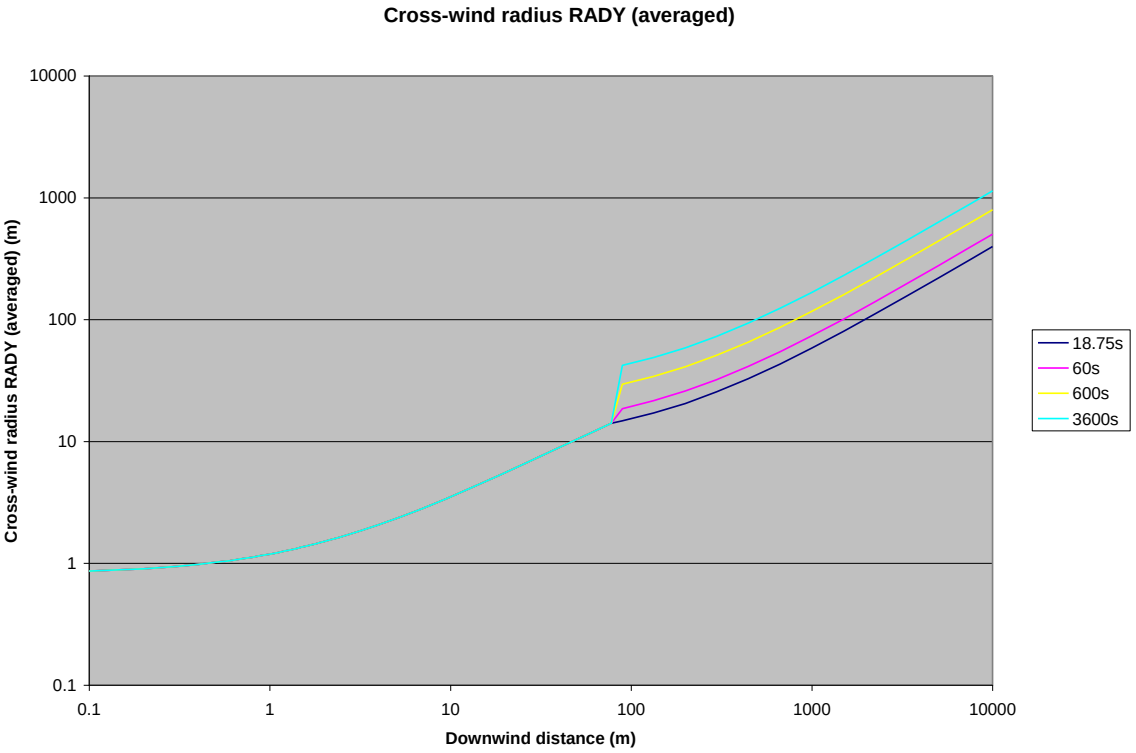

(b) cloud half-width R_y

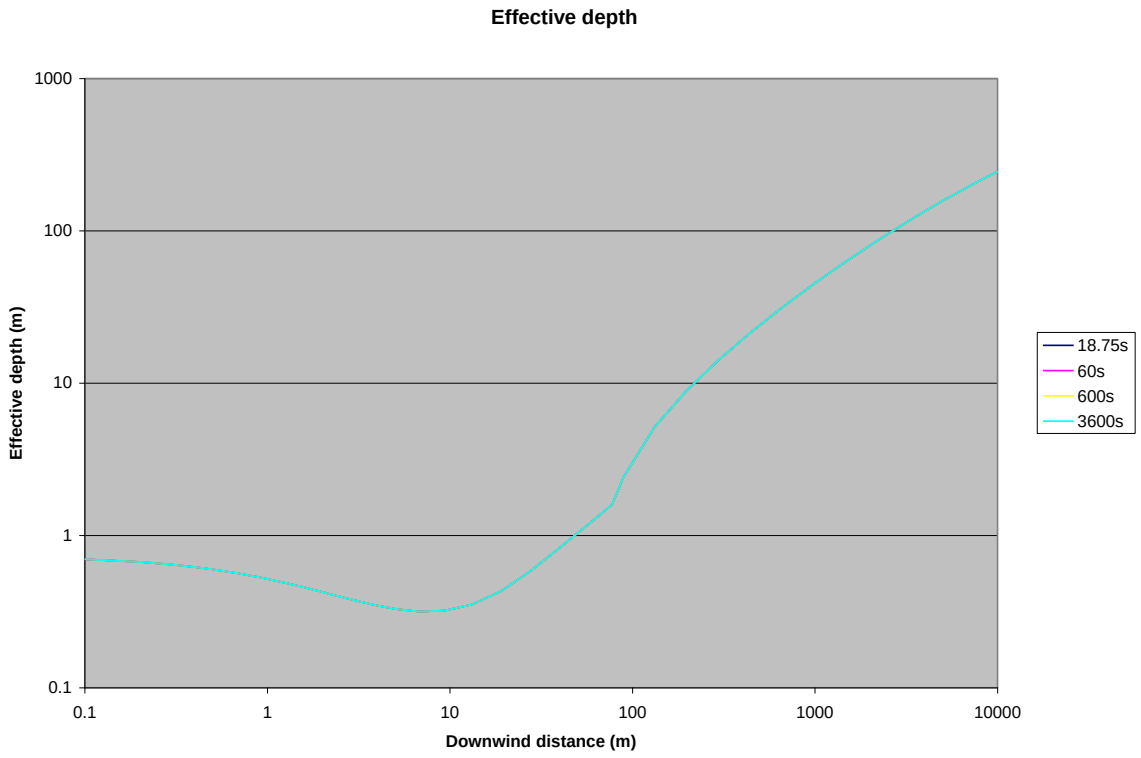

(c) effective depth $H_{eff}(1+h_d)$

Figure 5.8 **Variation of averaging time for heavy-gas base case**
[t_{av}^{core} = 18.75s; no phasing in of spread rate; averaging-time method B (old UDM)]
UDM predictions are included for averaging times t_{av} = 18.75, 60, 600, 3600 seconds.

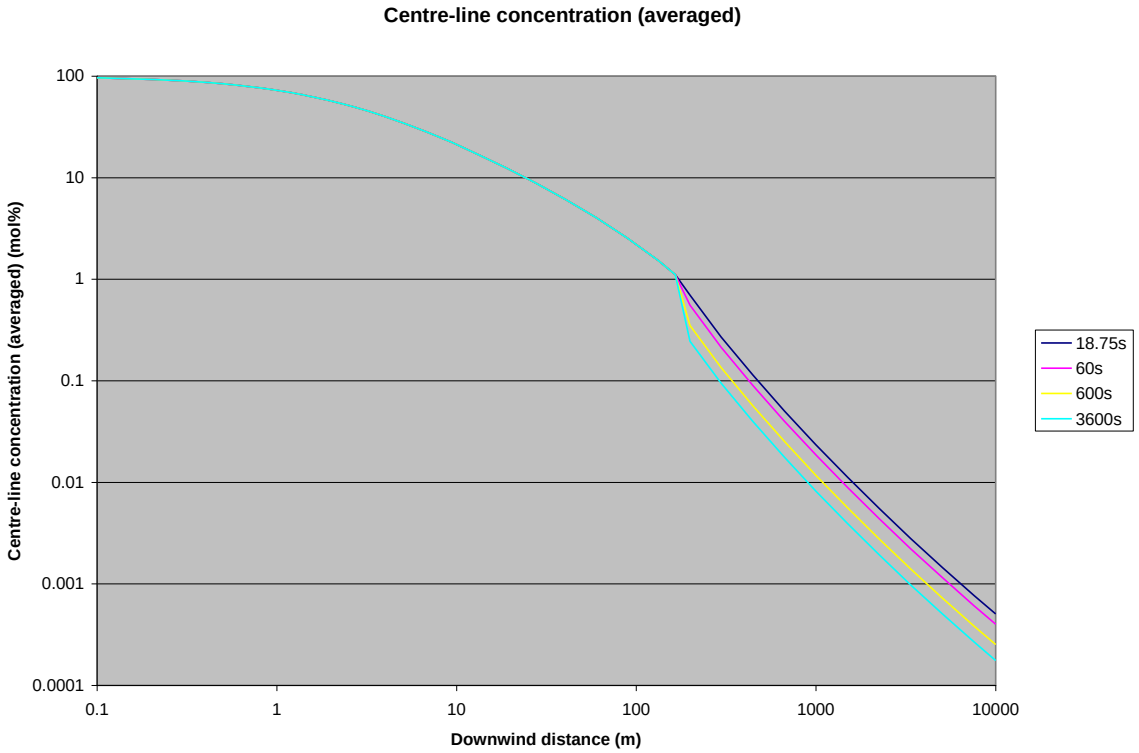

(a) centre-line concentration

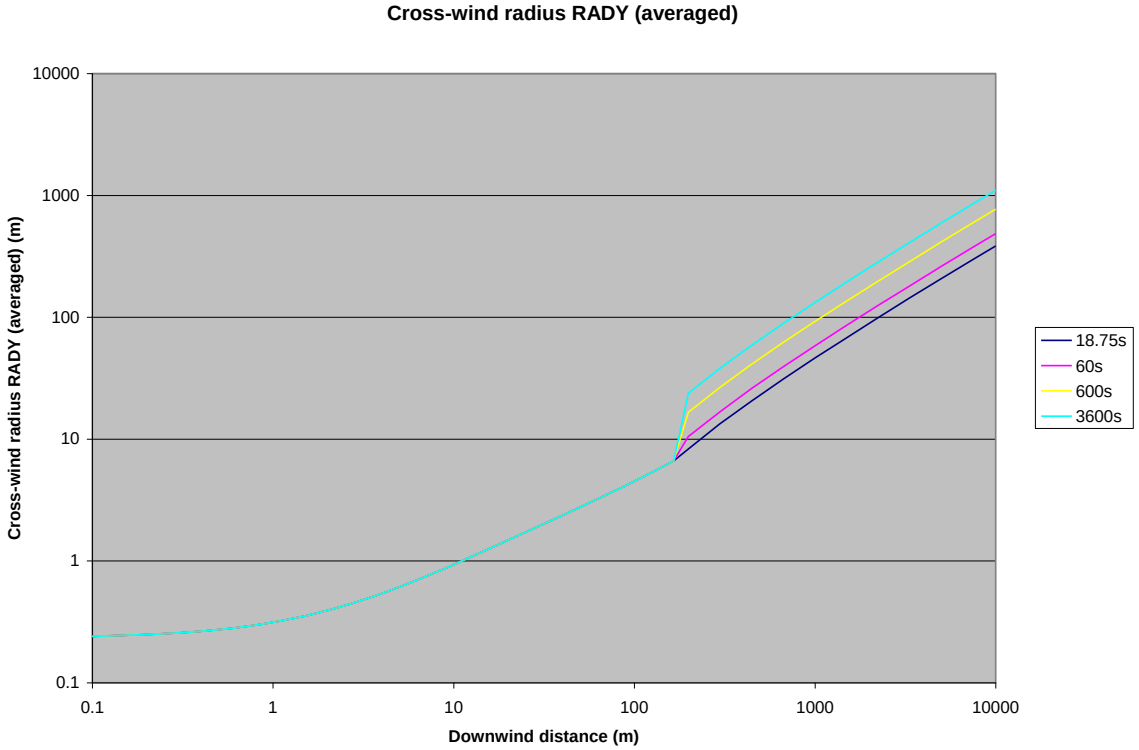

(b) cloud half-width R_y

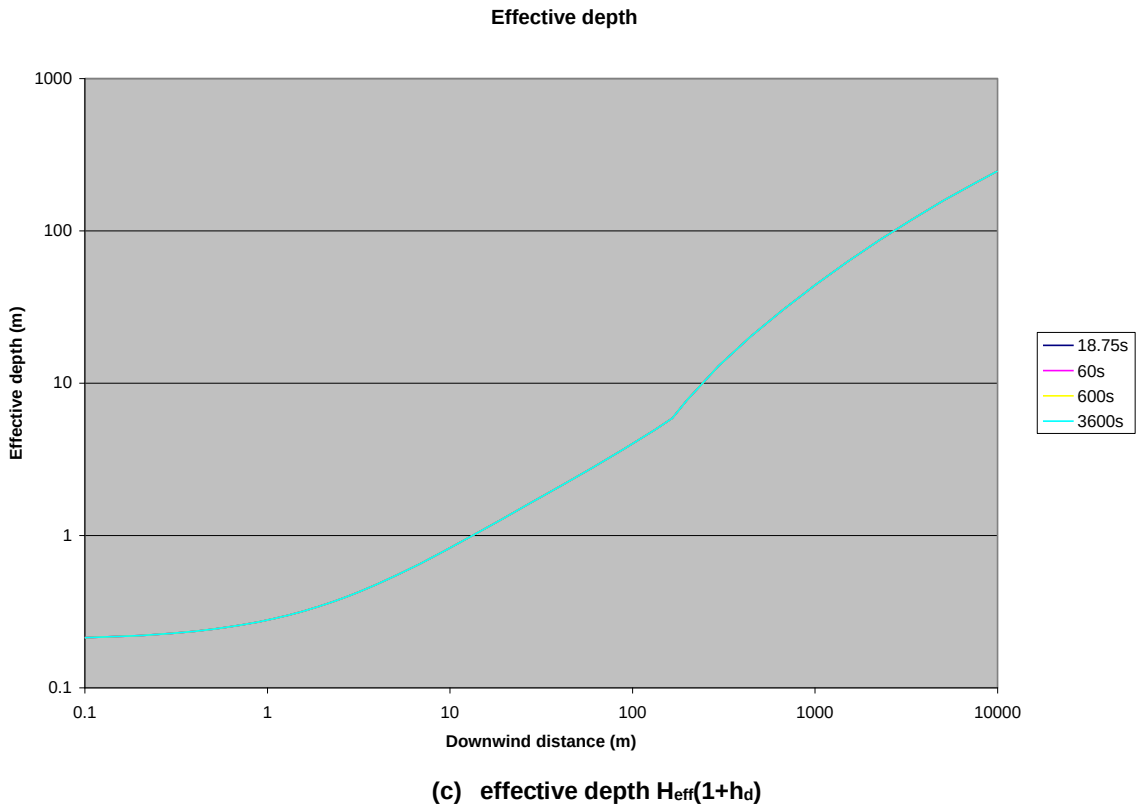

(c) effective depth $H_{eff}(1+h_d)$

Figure 5.9 **Variation of averaging time for elevated-jet base case**
[t_{av}^{core} = 18.75s; no phasing in of spread rate; averaging-time method B (old UDM)]
UDM predictions are included for averaging times t_{av} = 18.75, 60, 600, 3600 seconds.

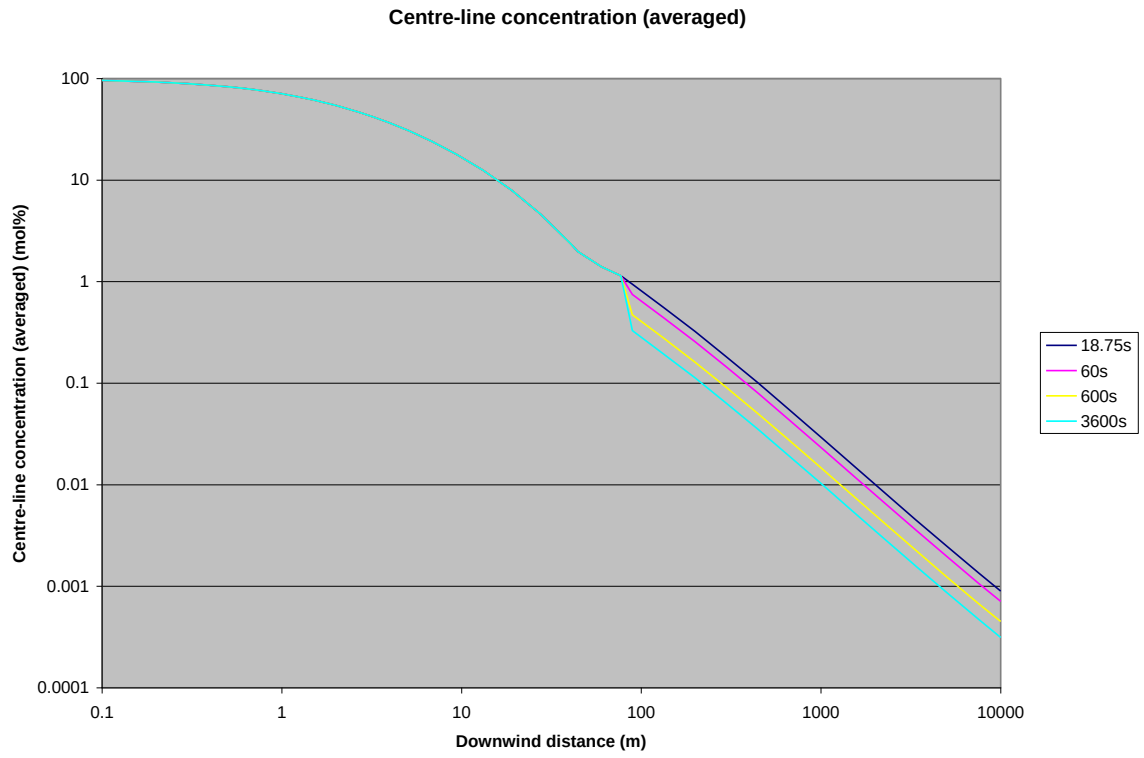

(a) centre-line concentration

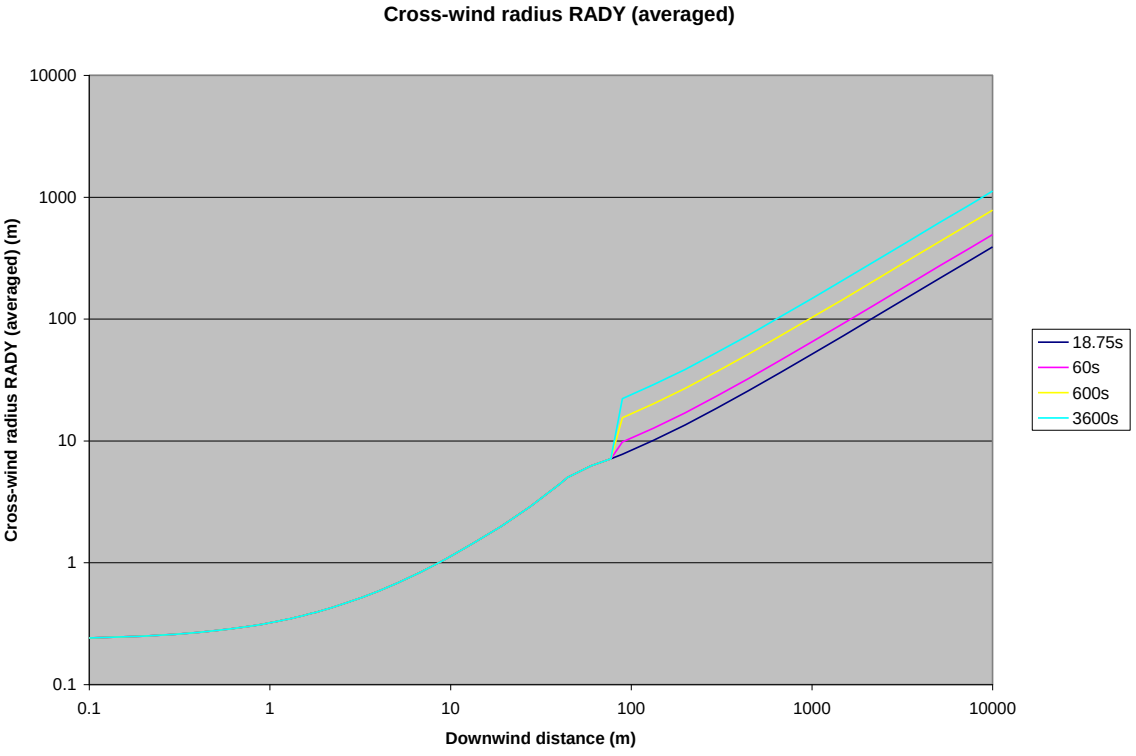

(b) cloud half-width R_y

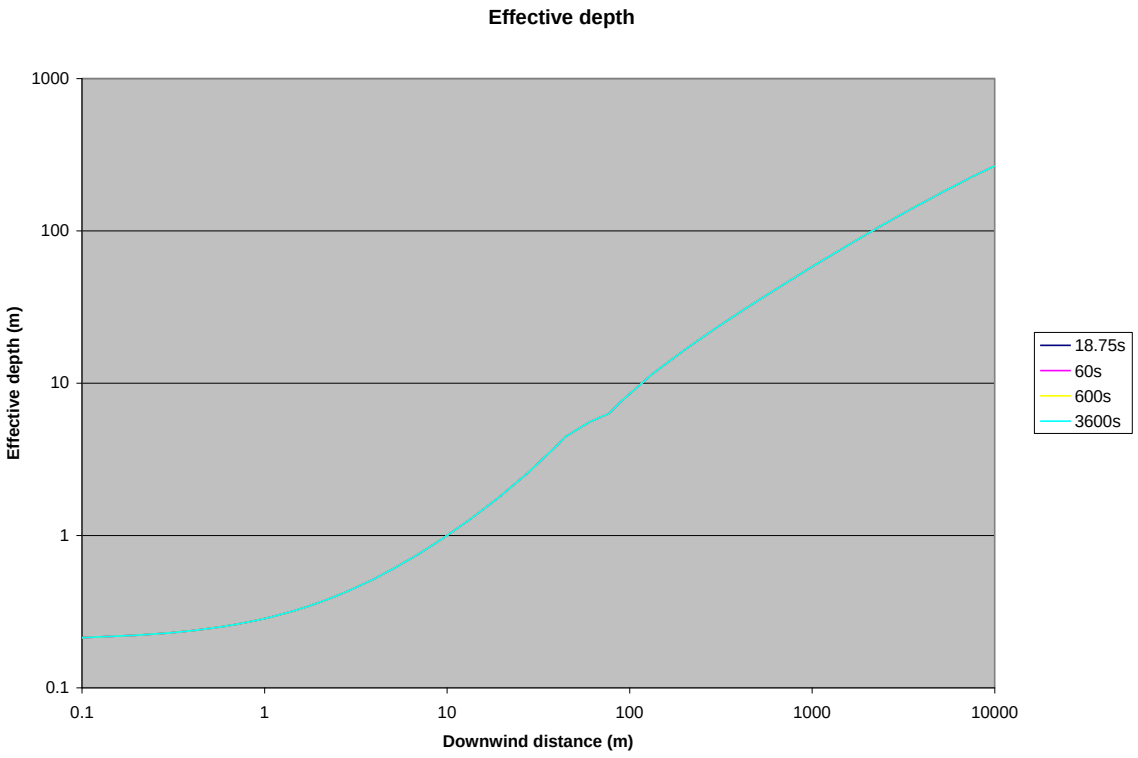

(c) effective depth $H_{eff}(1+h_d)$

Figure 5.10 **Variation of averaging time for touching-down jet base case**
[t_{av}^{core} = 18.75s; no phasing in of spread rate; averaging-time method B (old UDM)]
UDM predictions are included for averaging times t_{av} = 18.75, 60, 600, 3600 seconds.

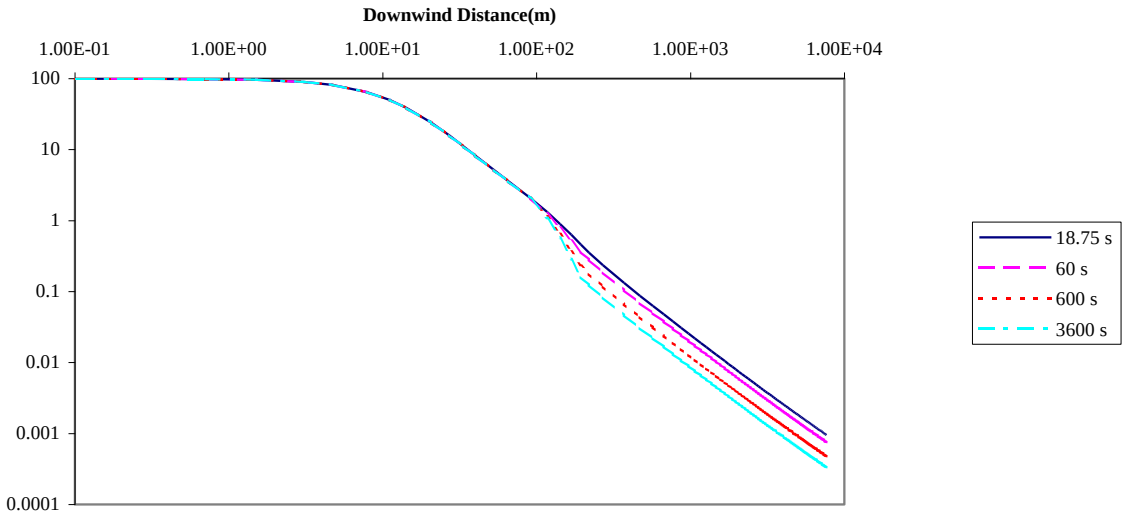

(a) centre-line concentration

Cloud Radius - RADY

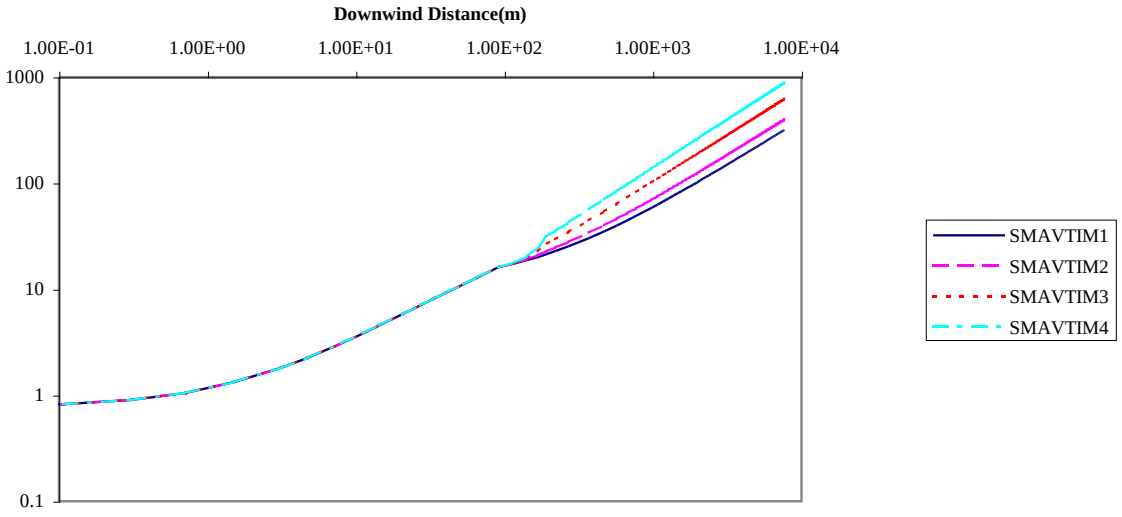

(b) cloud half-width R_y

Figure 5.11 **Variation of averaging time for heavy-gas base case**
[t_{av}^{core} = 18.75s; no phasing in of spread rate; averaging-time method C (improved width)]
UDM predictions are included for averaging times t_{av} = 18.75, 60, 600, 3600 seconds.

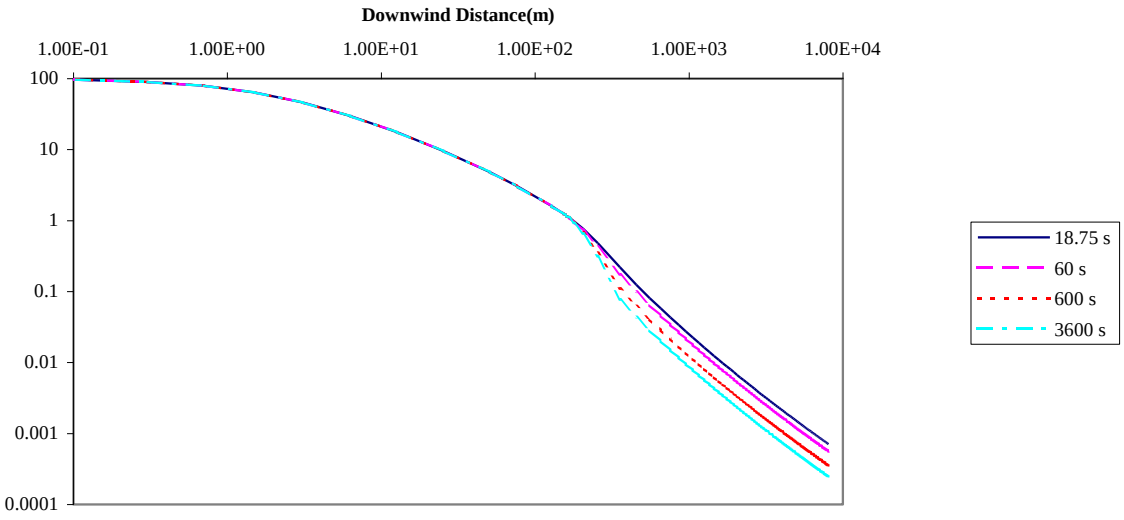

(a) centre-line concentration

Effective half-width

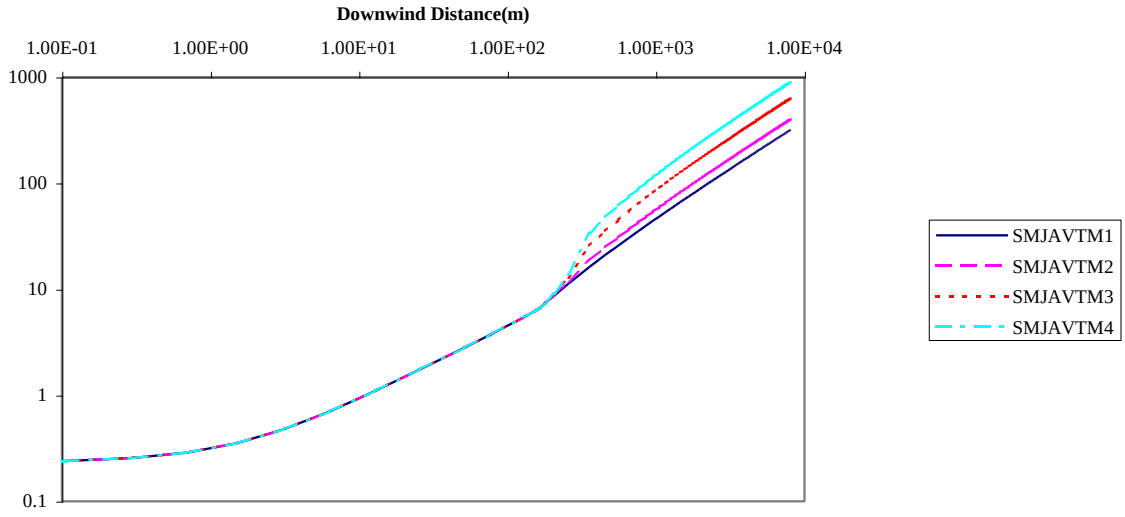

(b) cloud half-width R_y

Figure 5.12 **Variation of averaging time for elevated-jet base case**
[t_{av}^{core} = 18.75s; no phasing in of spread rate; averaging-time method C (improved width)]
UDM predictions are included for averaging times t_{av} = 18.75, 60, 600, 3600 seconds.

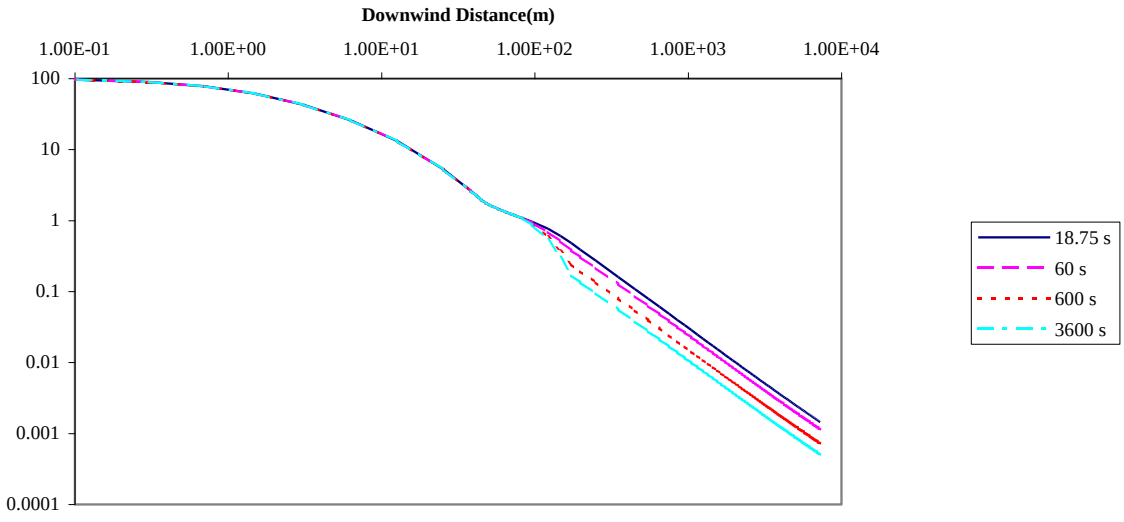

(a) centre-line concentration

Effective half-width

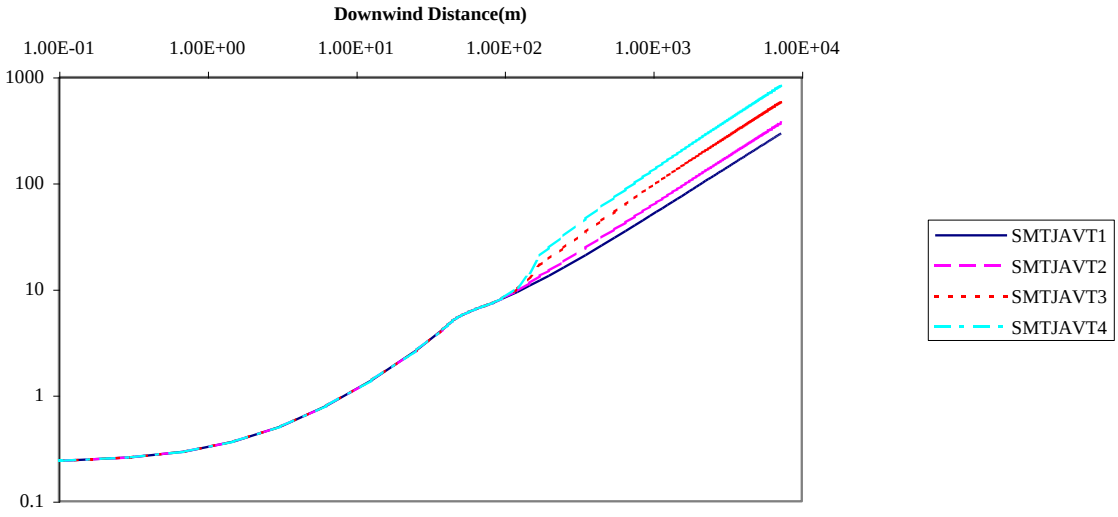

(b) cloud half-width R_y

Figure 5.13 **Variation of averaging time for touching-down jet base case**
[t_{av}^{core} = 18.75s; no phasing in of spread rate; averaging-time method C (improved width)] UDM predictions are included for averaging times t_{av} = 18.75, 60, 600, 3600 seconds.

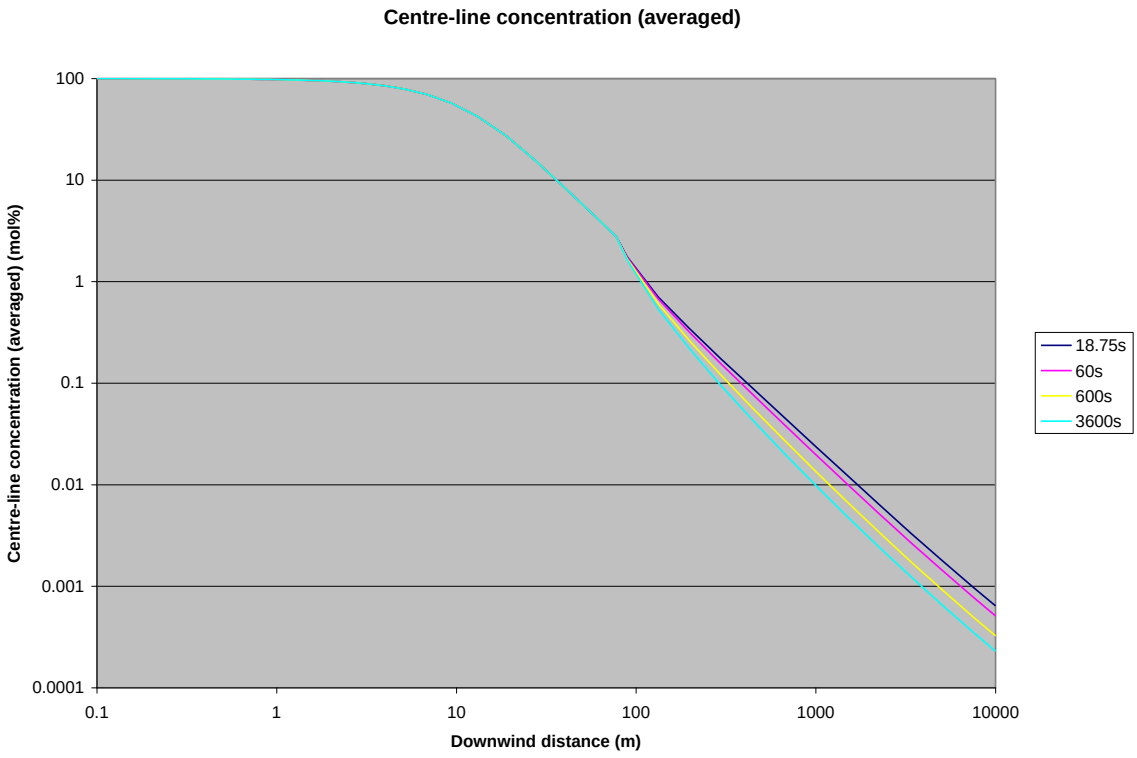

(a) centre-line concentration

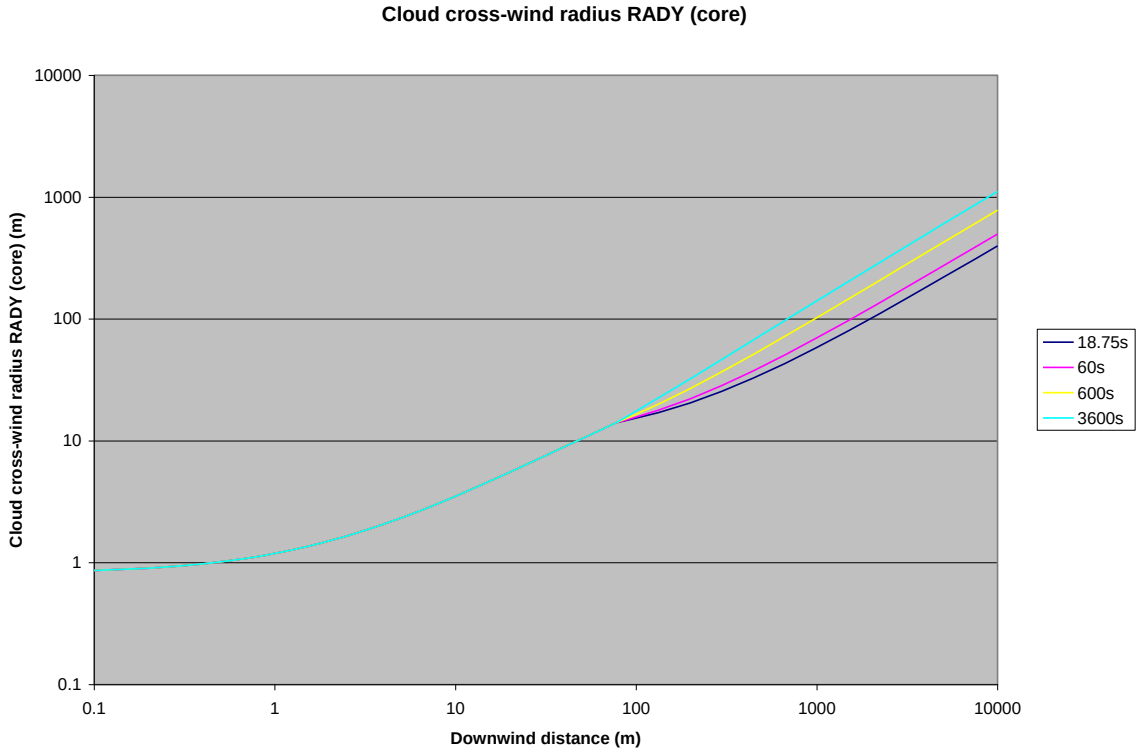

(b) cloud half-width R_y

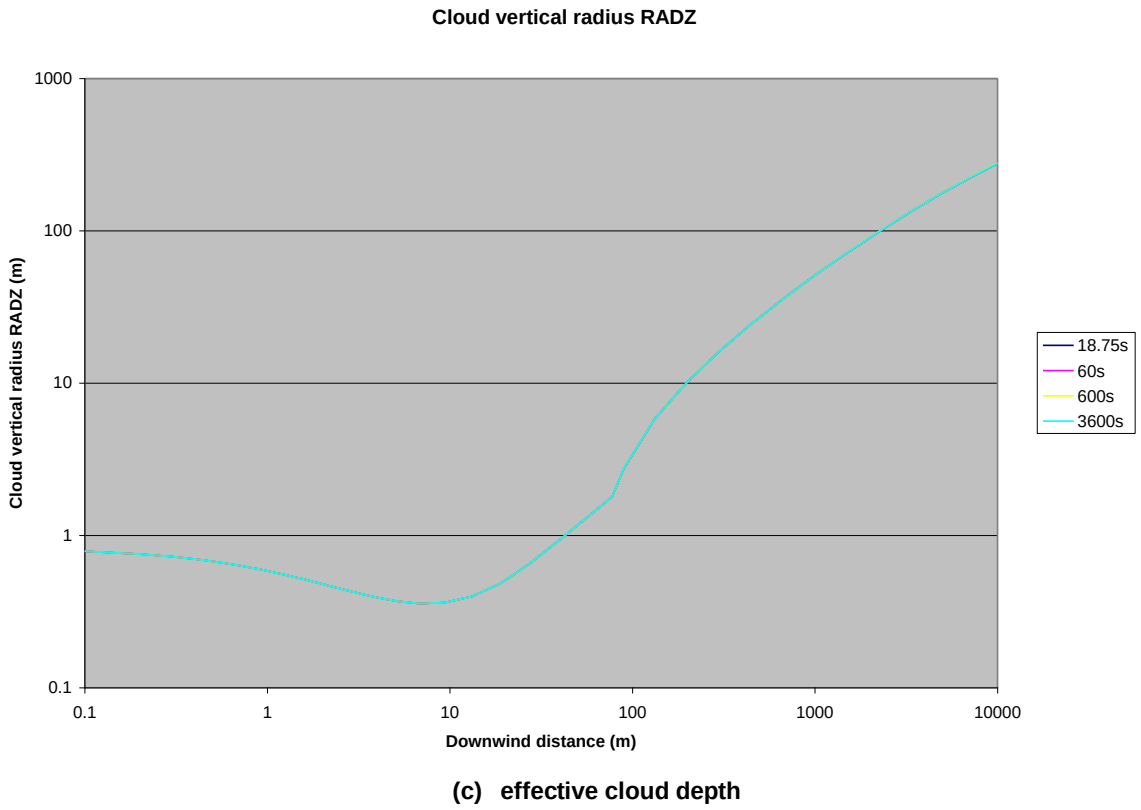

(c) effective cloud depth

Figure 5.14 **Variation of averaging time for heavy-gas base case**
[$t_{av}^{core} = t_{av}$; no phasing in of spread rate; method A (no averaging time correction)] UDM predictions are included for averaging times t_{av} = 18.75, 60, 600, 3600 seconds.

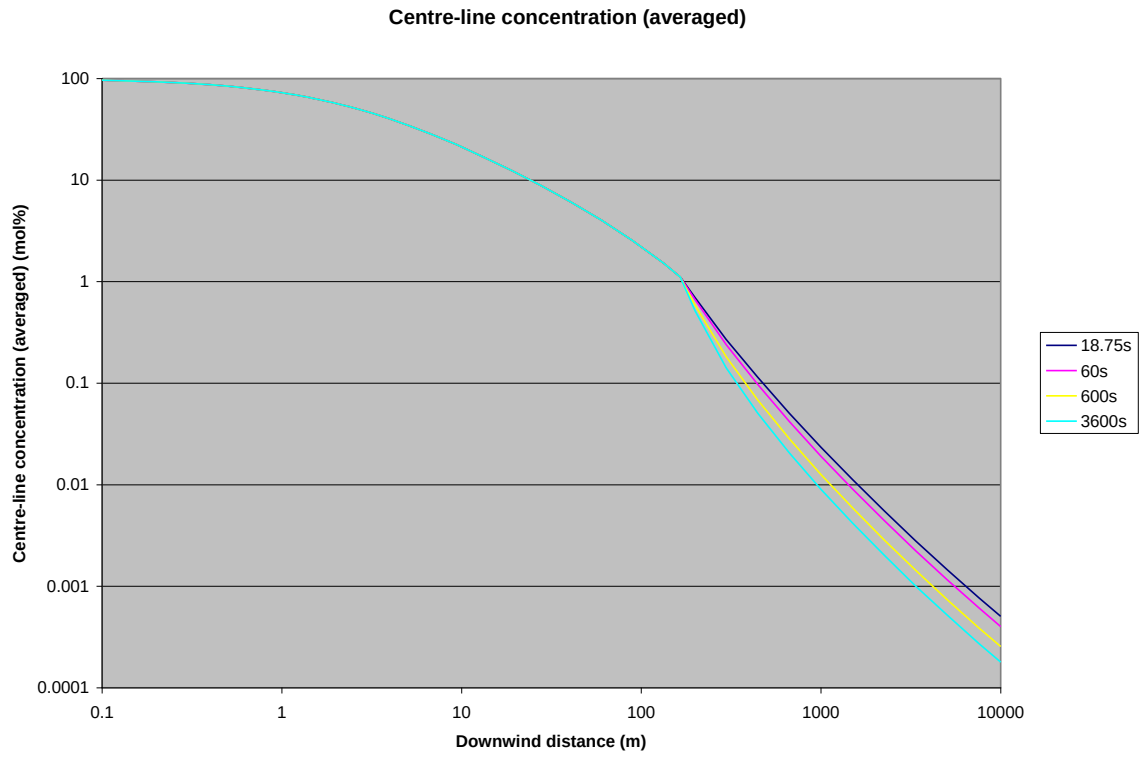

(a) centre-line concentration

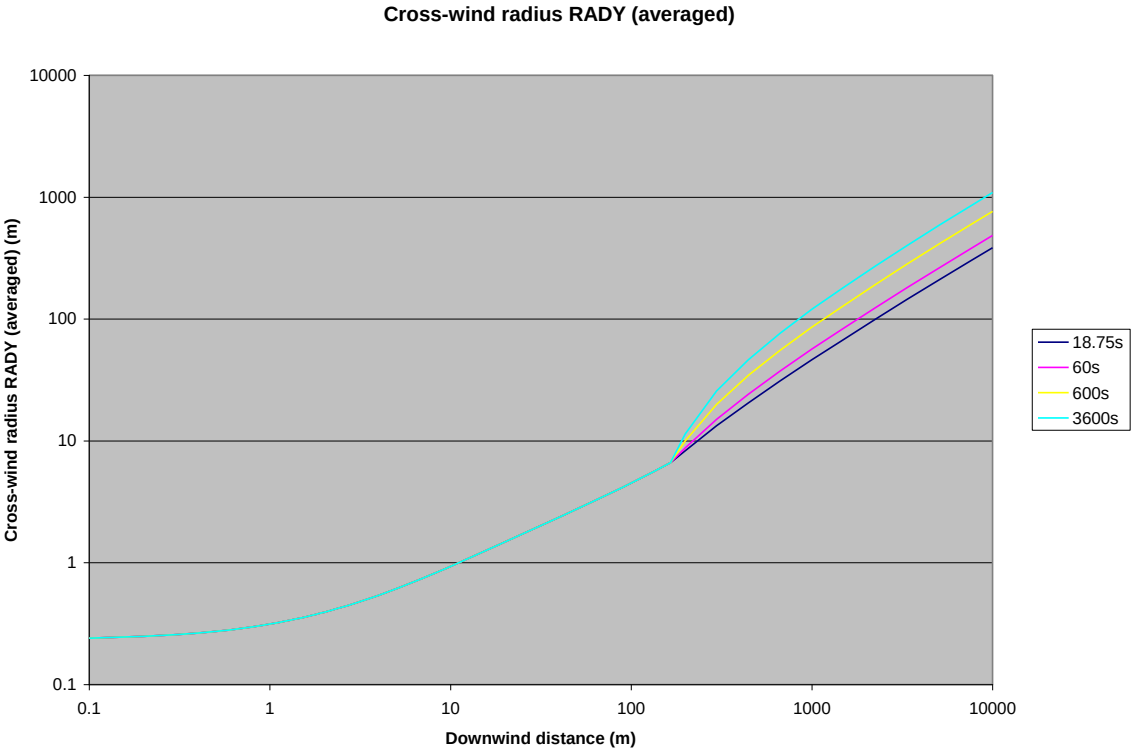

(b) cloud half-width R_y

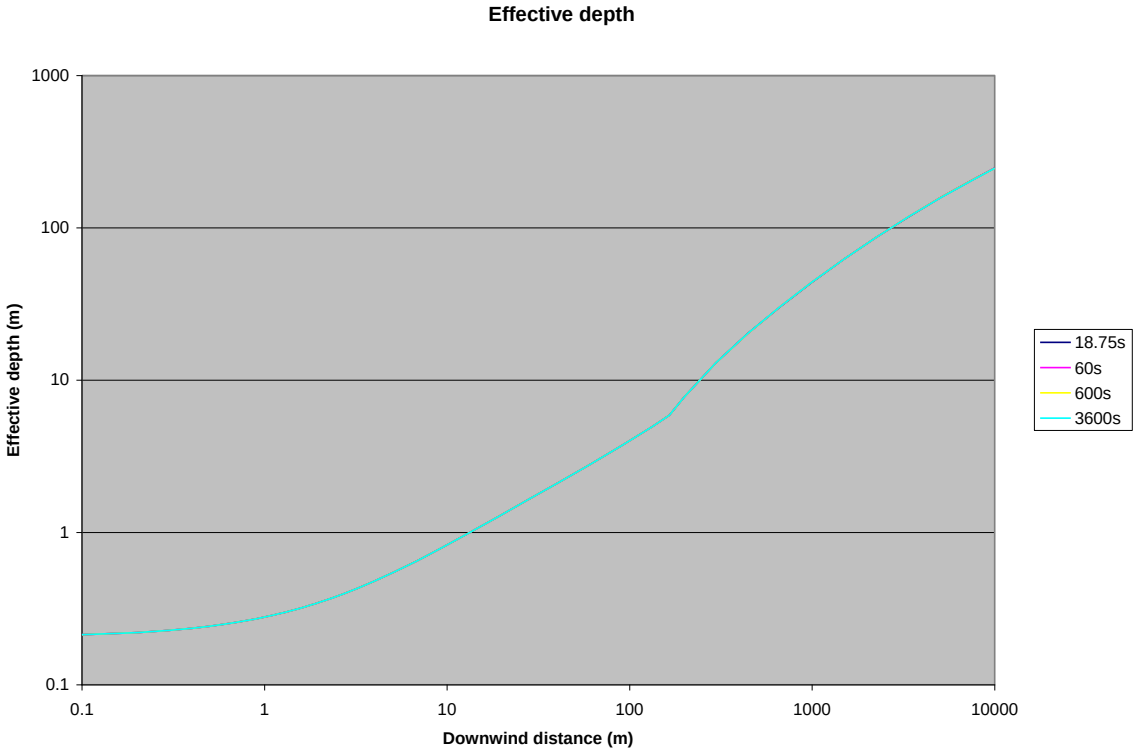

(c) effective cloud depth $H_{eff}(1+h_d)$

Figure 5.15 **Variation of averaging time for elevated-jet base case**
[t_{av}^{core} = t_{av}; no phasing in of spread rate; method A (no averaging time correction)]
UDM predictions are included for averaging times t_{av} = 18.75, 60, 600, 3600 seconds.

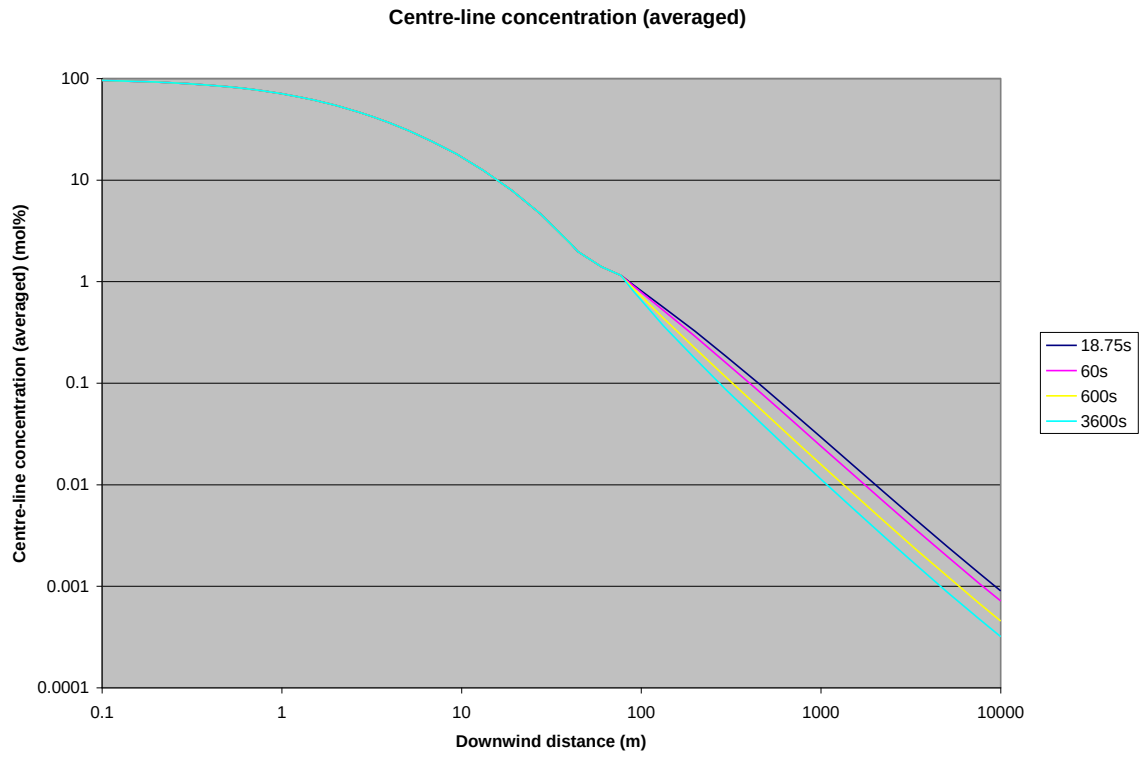

(a) centre-line concentration

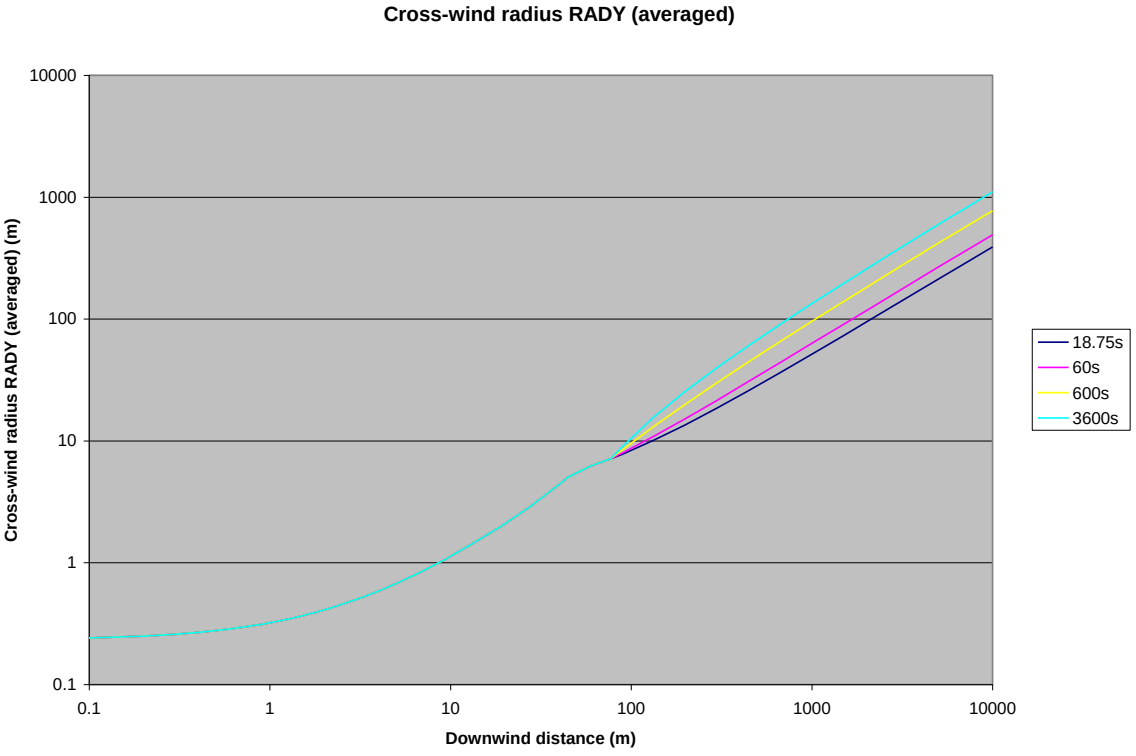

(b) cloud half-width R_y

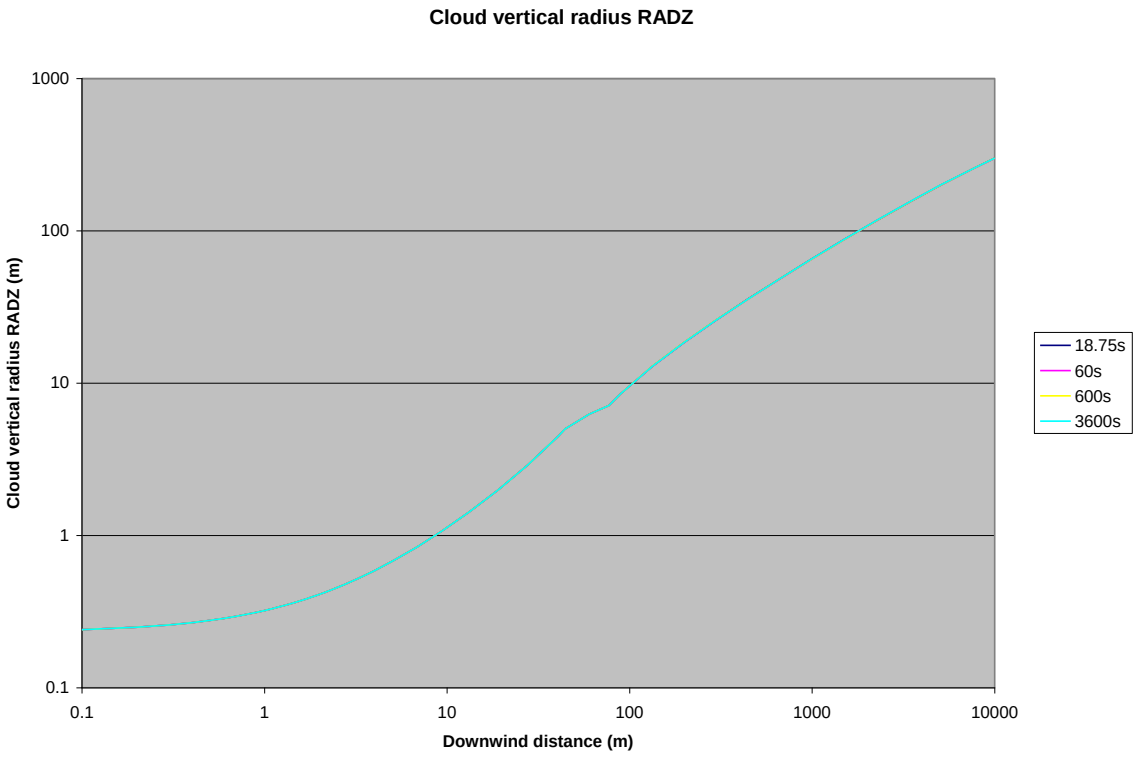

(c) effective cloud depth $H_{eff}(1+h_d)$

Figure 5.16 **Variation of averaging time for touching-down jet base case**
[$t_{av}^{core} = t_{av}$; no phasing in of spread rate; method A (no averaging time correction)]
UDM predictions are included for averaging times t_{av} = 18.75, 60, 600, 3600 seconds.

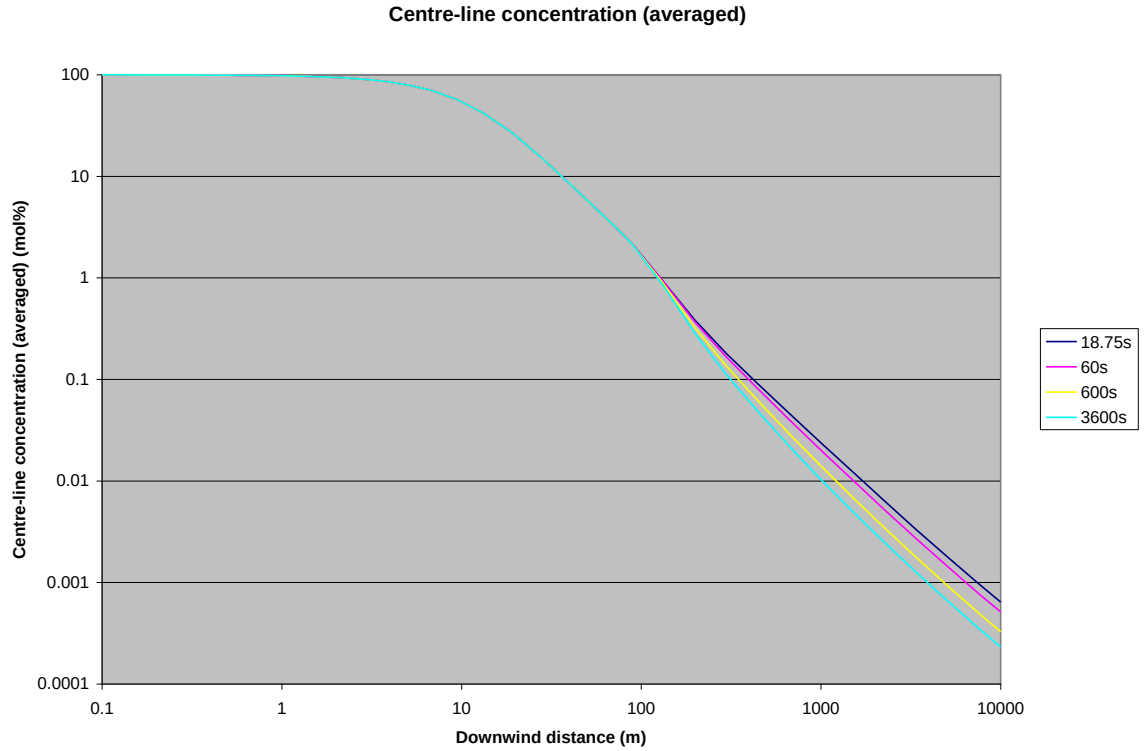

(a) centre-line concentration

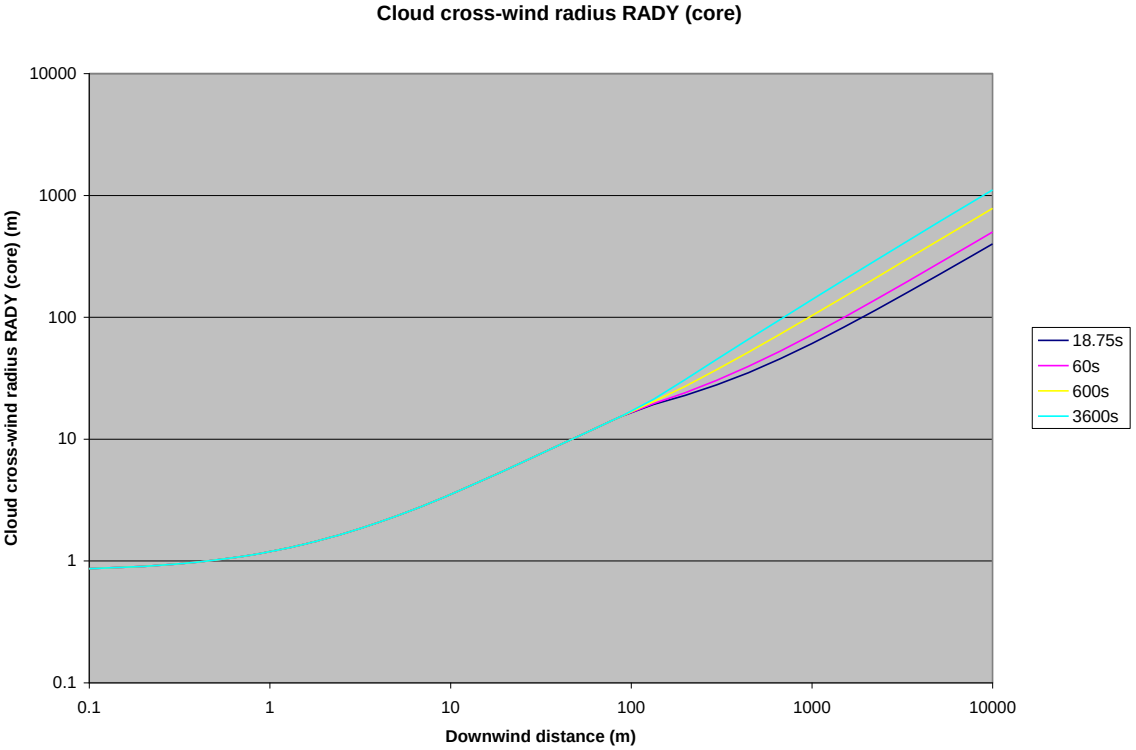

(b) cloud half-width R_y

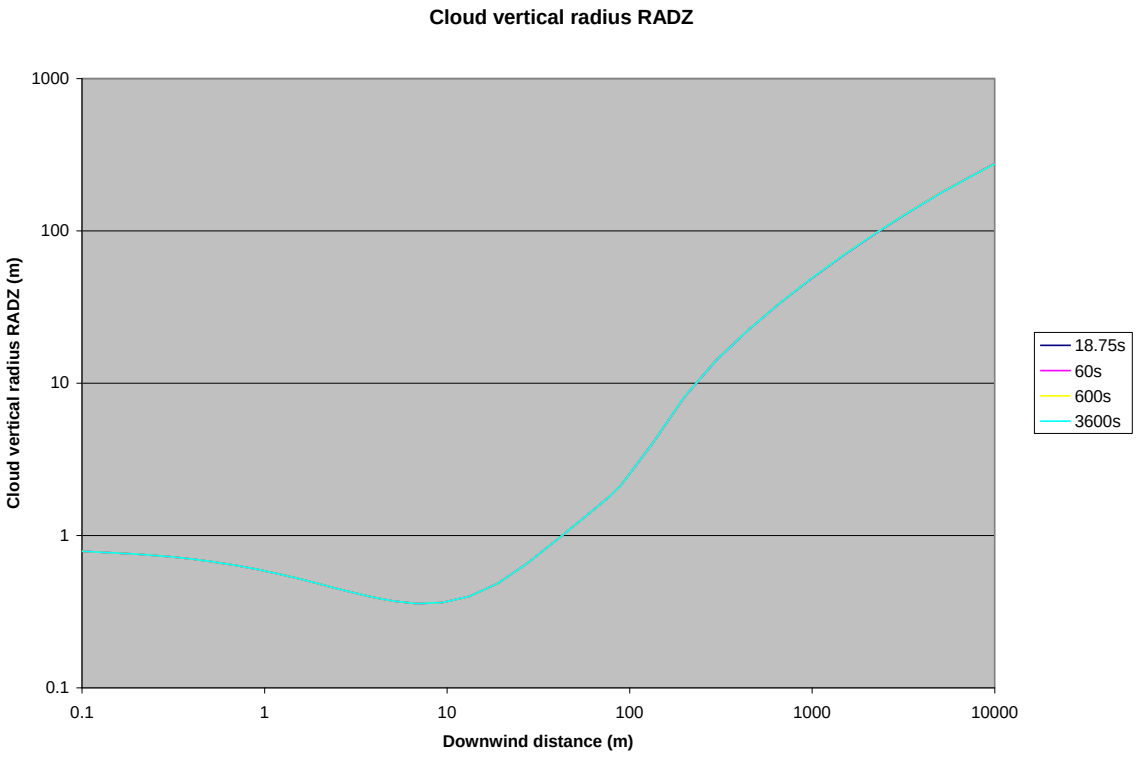

(c) effective cloud depth $H_{eff}(1+h_d)$

Figure 5.17 **Variation of averaging time for heavy-gas base case**
[$t_{av}^{core} = t_{av}$; phase in spread rate; method A (no averaging time correction)]
UDM predictions are included for averaging times t_{av} = 18.75, 60, 600, 3600 seconds.

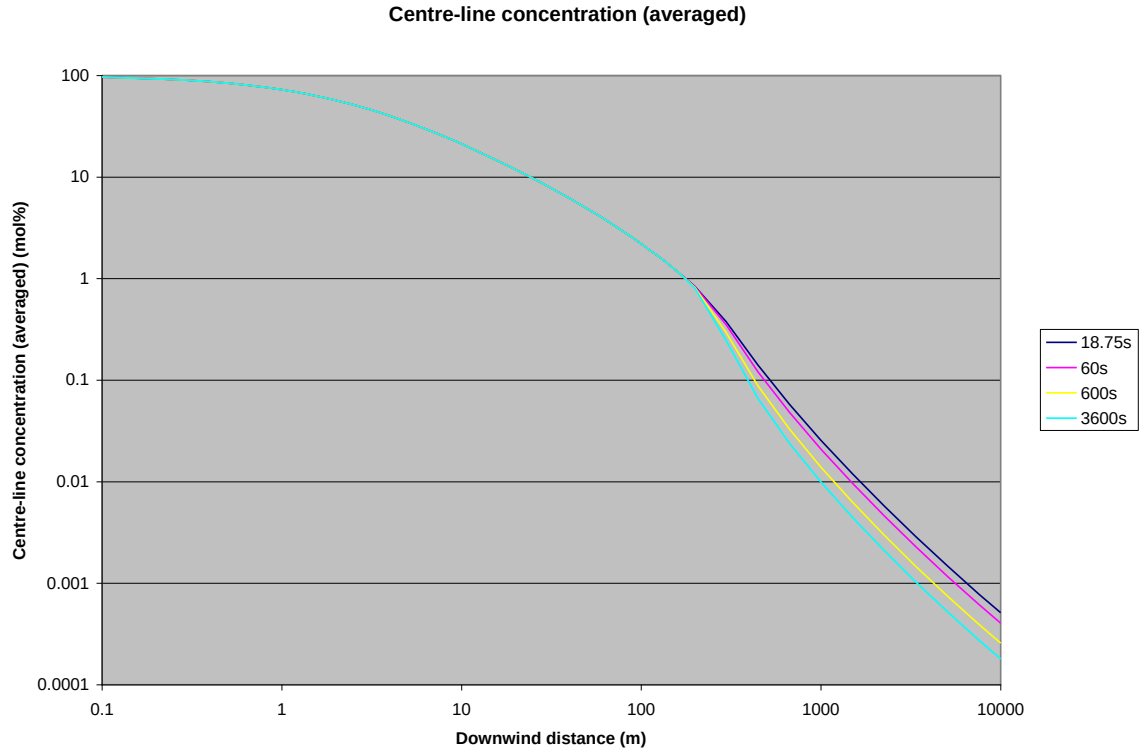

(a) centre-line concentration

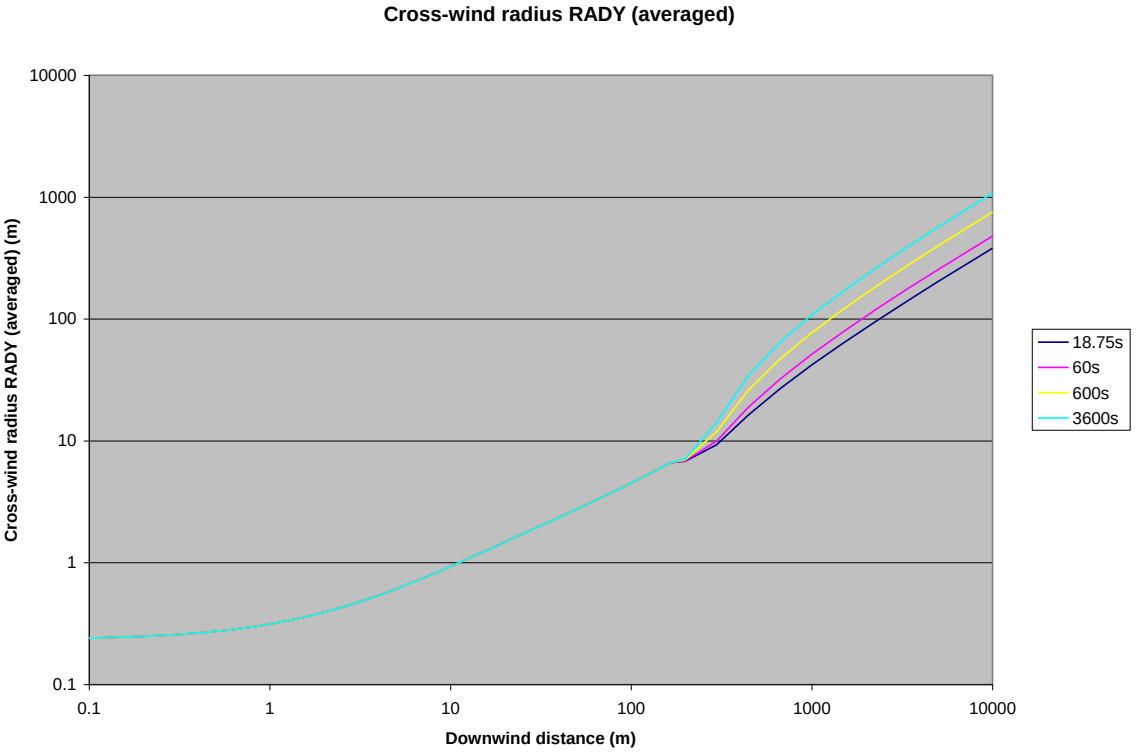

(b) cloud half-width R_y

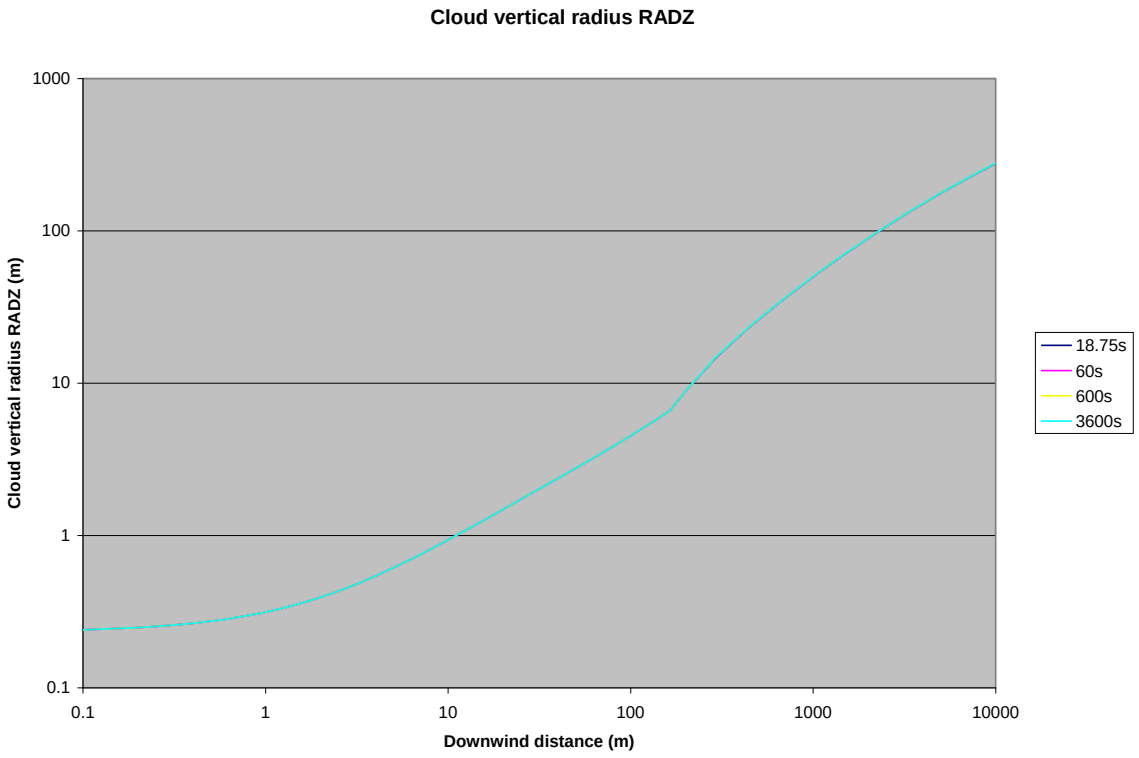

(c) effective cloud depth $H_{eff}(1+h_d)$

Figure 5.18 **Variation of averaging time for elevated-jet base case**
[$t_{av}^{core} = t_{av}$; phase in spread rate; method A (no averaging time correction)]
UDM predictions are included for averaging times t_{av} = 18.75, 60, 600, 3600 seconds.

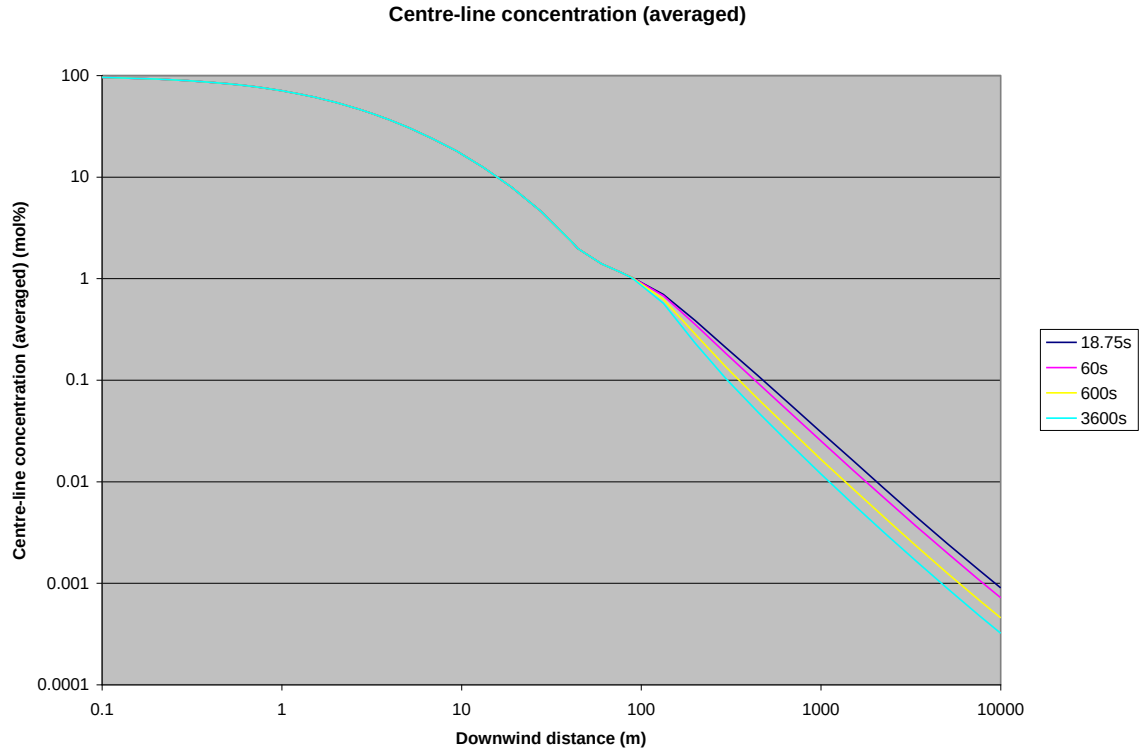

(a) centre-line concentration

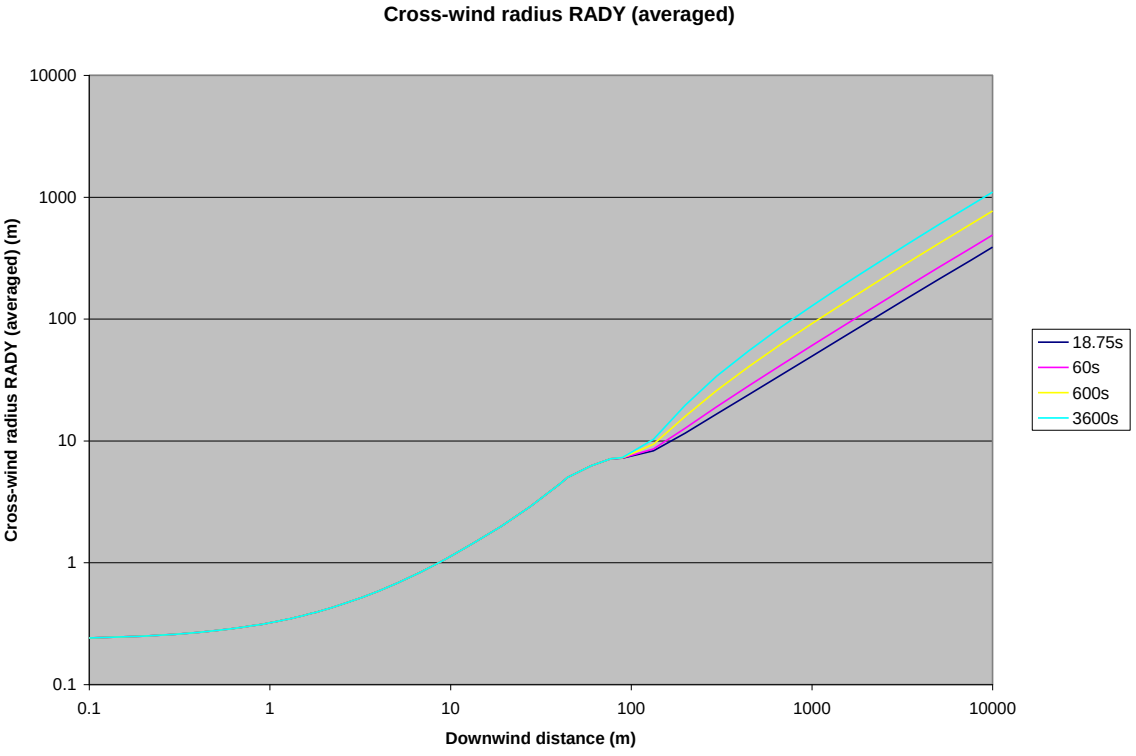

(b) cloud half-width R_y

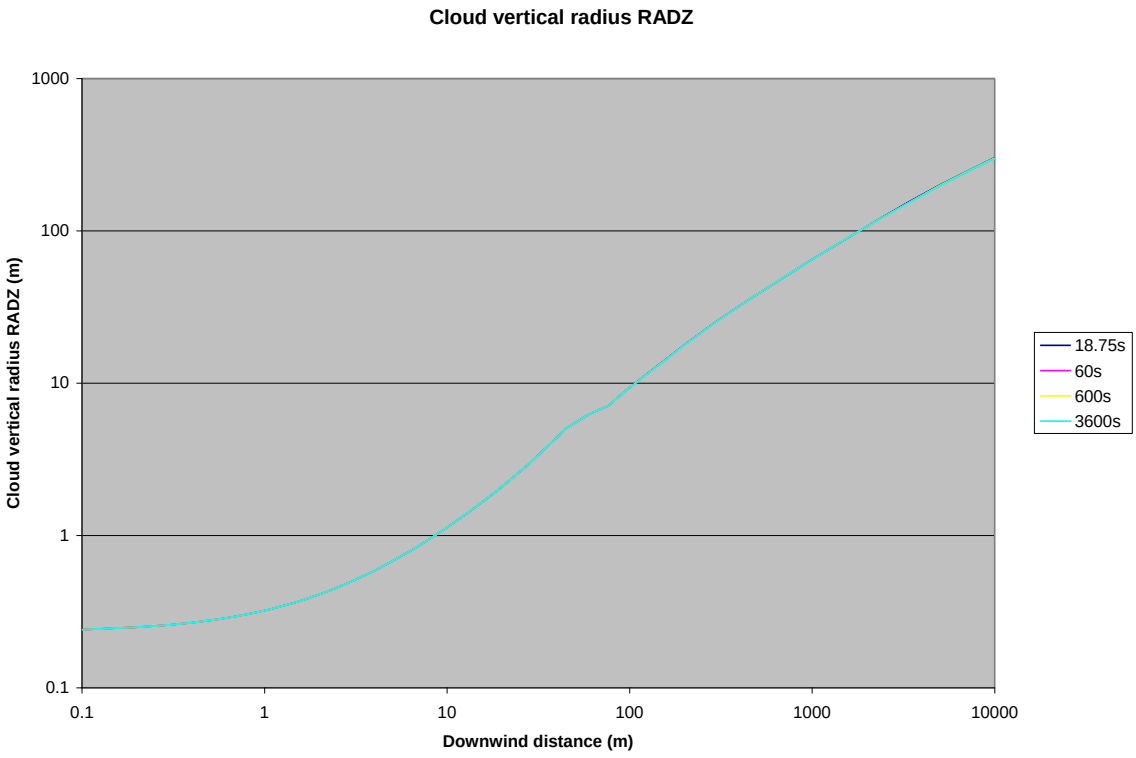

(c) effective cloud depth $H_{eff}(1+h_d)$

Figure 5.19 **Variation of averaging time for touching-down jet base case**
[$t_{av}^{core} = t_{av}$; phase in spread rate; method A (no averaging time correction)]
UDM predictions are included for averaging times t_{av} = 18.75, 60, 600, 3600 seconds.

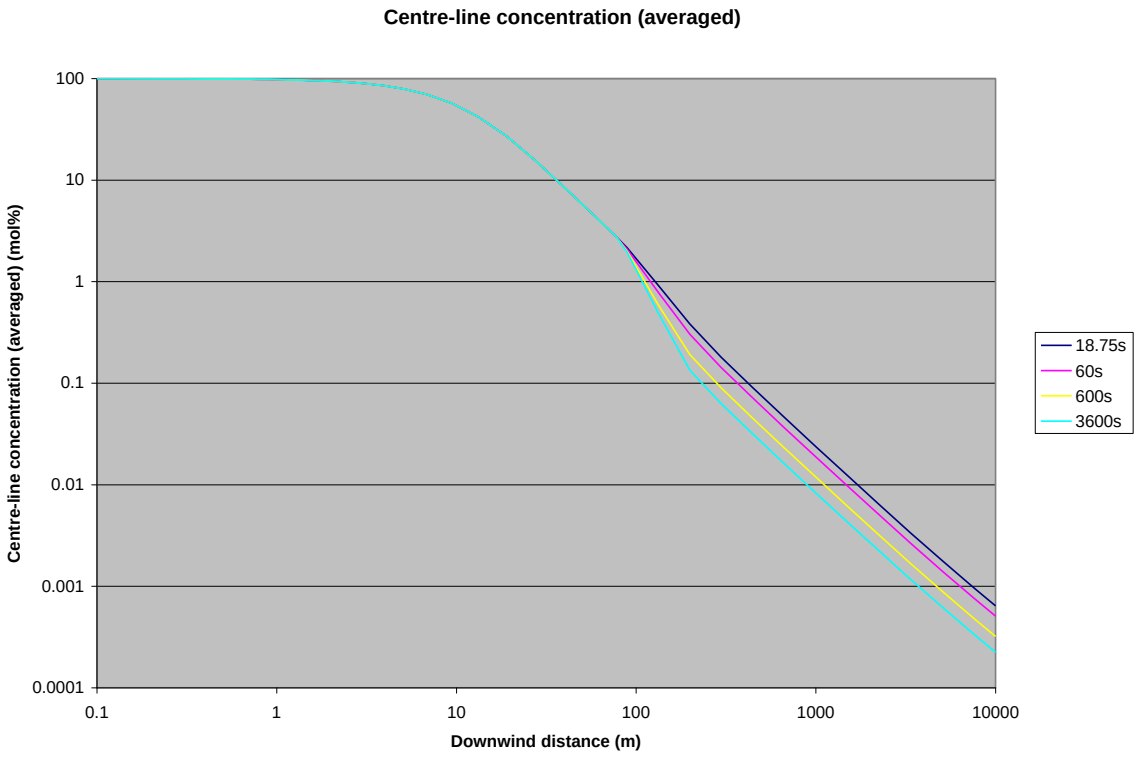

(a) centre-line concentration

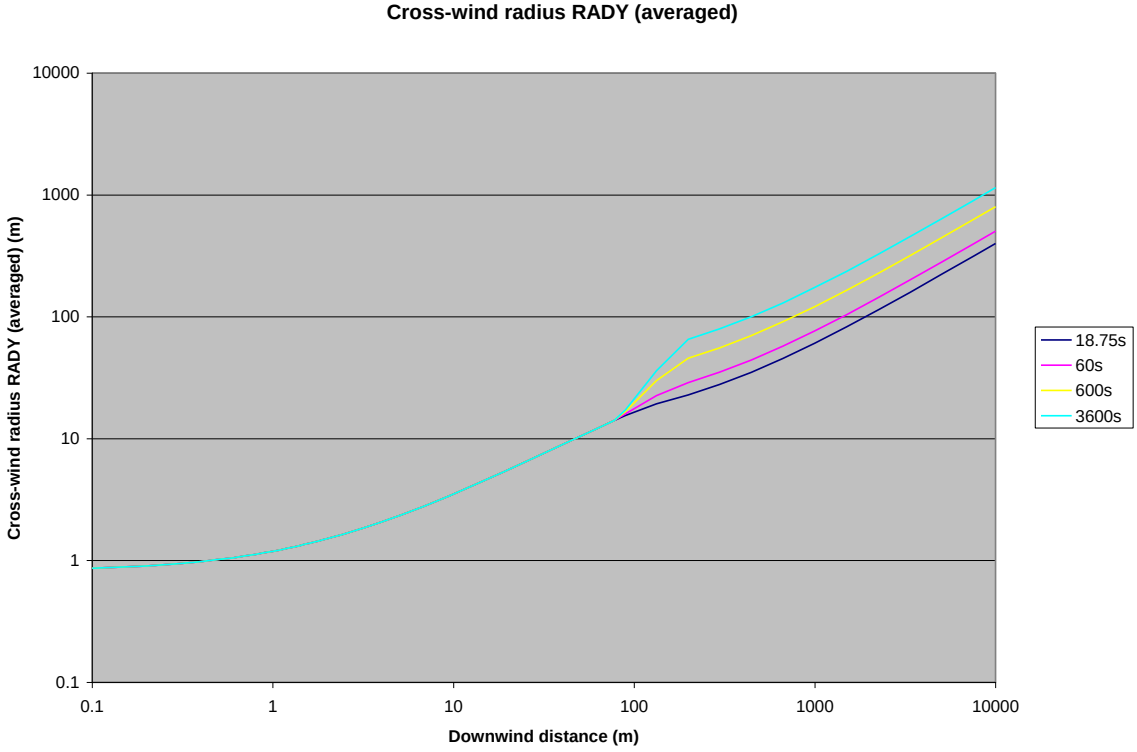

(b) cloud half-width R_y

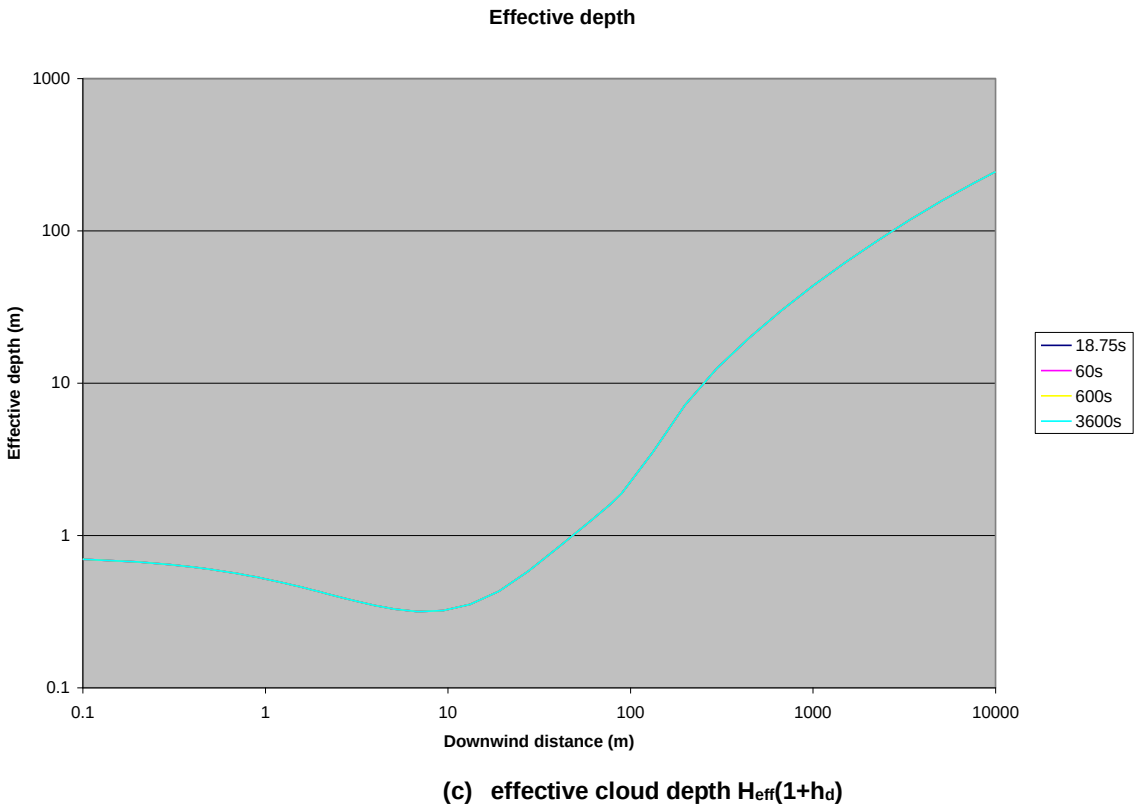

(c) effective cloud depth $H_{eff}(1+h_d)$

Figure 5.20 **Variation of averaging time for heavy-gas base case**
[t_{av}^{core} = 18.75; phase in spread rate; averaging-time method B (old UDM)]
UDM predictions are included for averaging times t_{av} = 18.75, 60, 600, 3600 seconds.

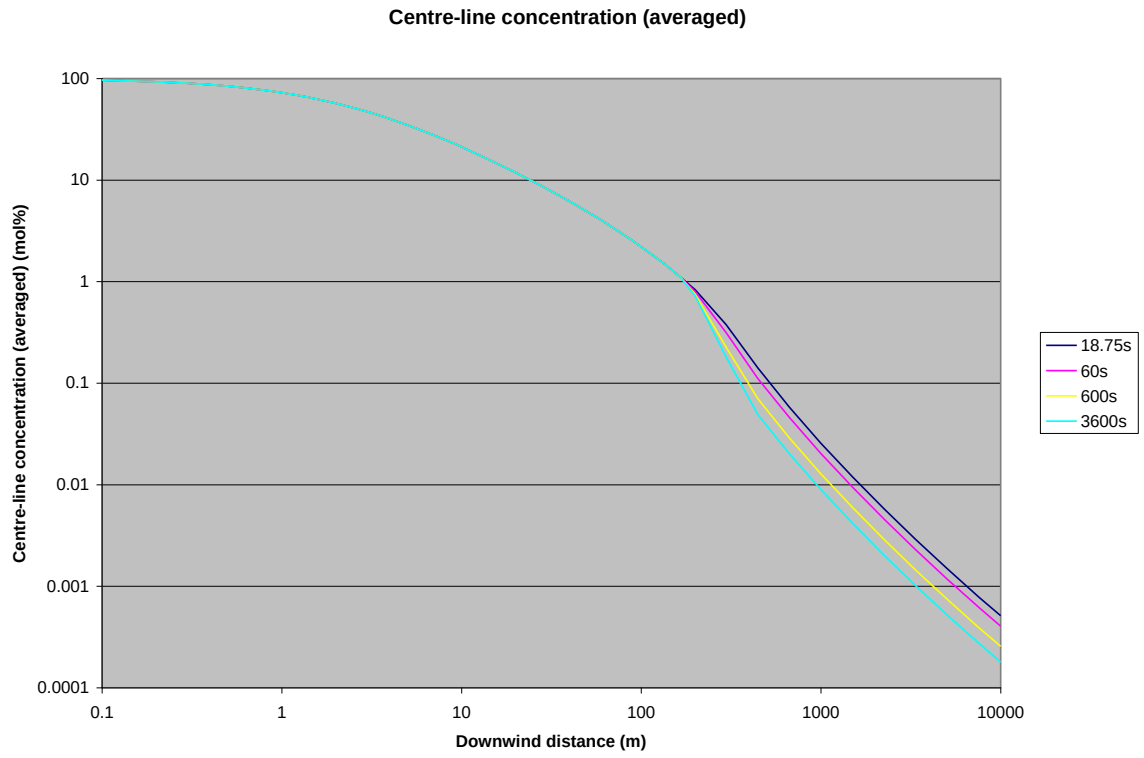

(a) centre-line concentration

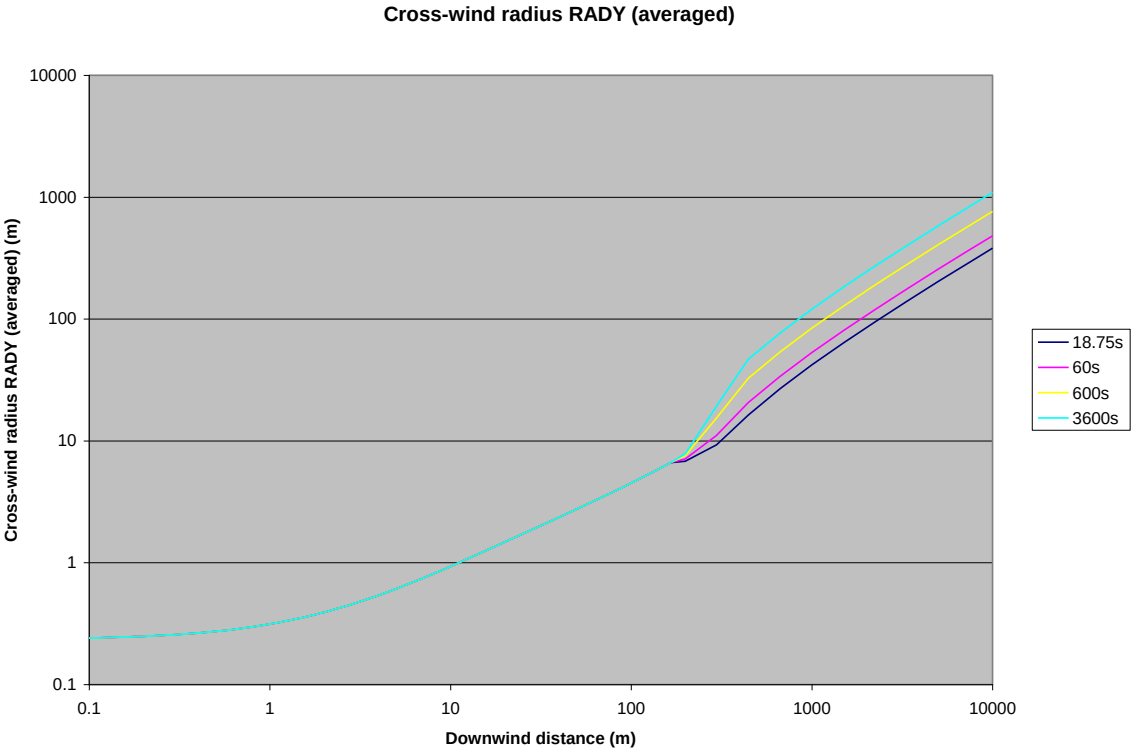

(b) cloud half-width R_y

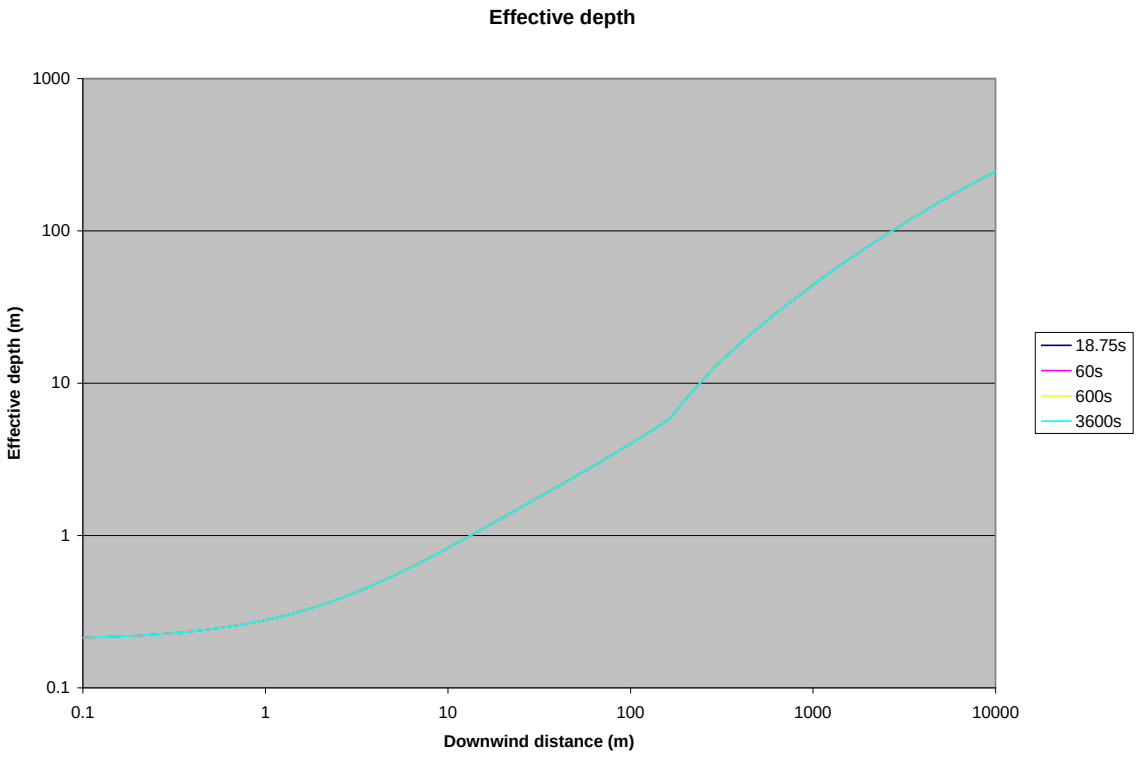

(c) effective cloud depth $H_{eff}(1+h_d)$

Figure 5.21 **Variation of averaging time for elevated-jet base case**
[t_{av}^{core} = 18.75; phase in spread rate; averaging-time method B (old UDM)]
UDM predictions are included for averaging times t_{av} = 18.75, 60, 600, 3600 seconds.

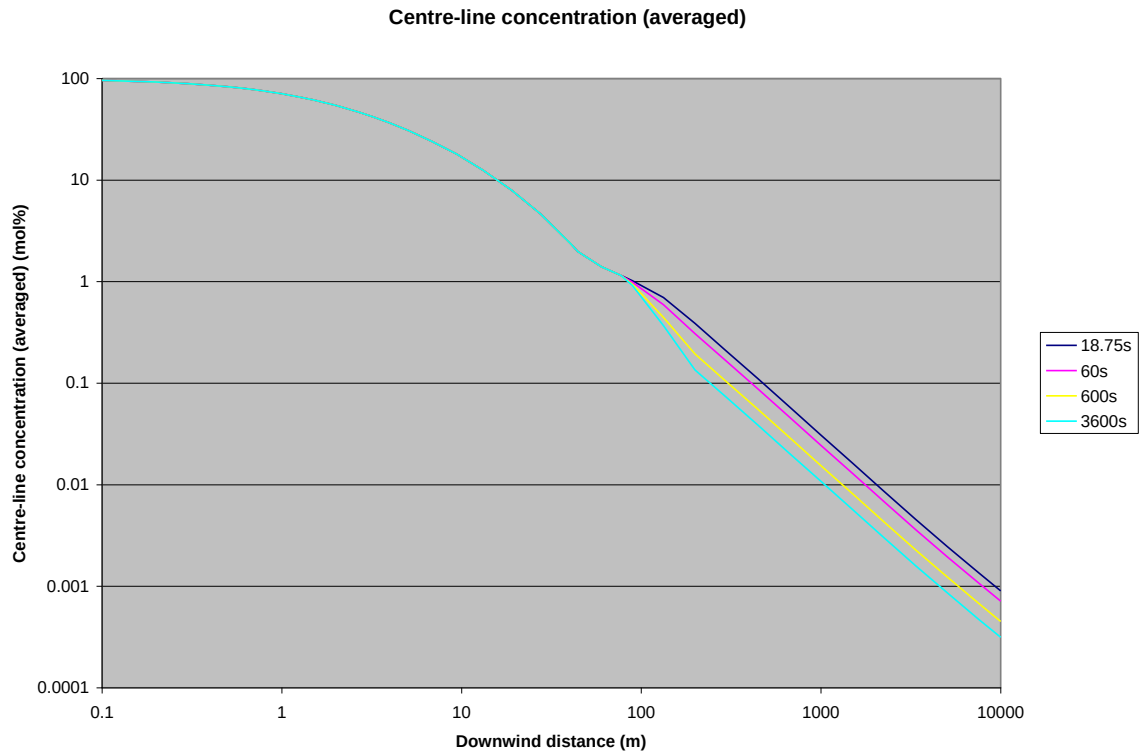

(a) centre-line concentration

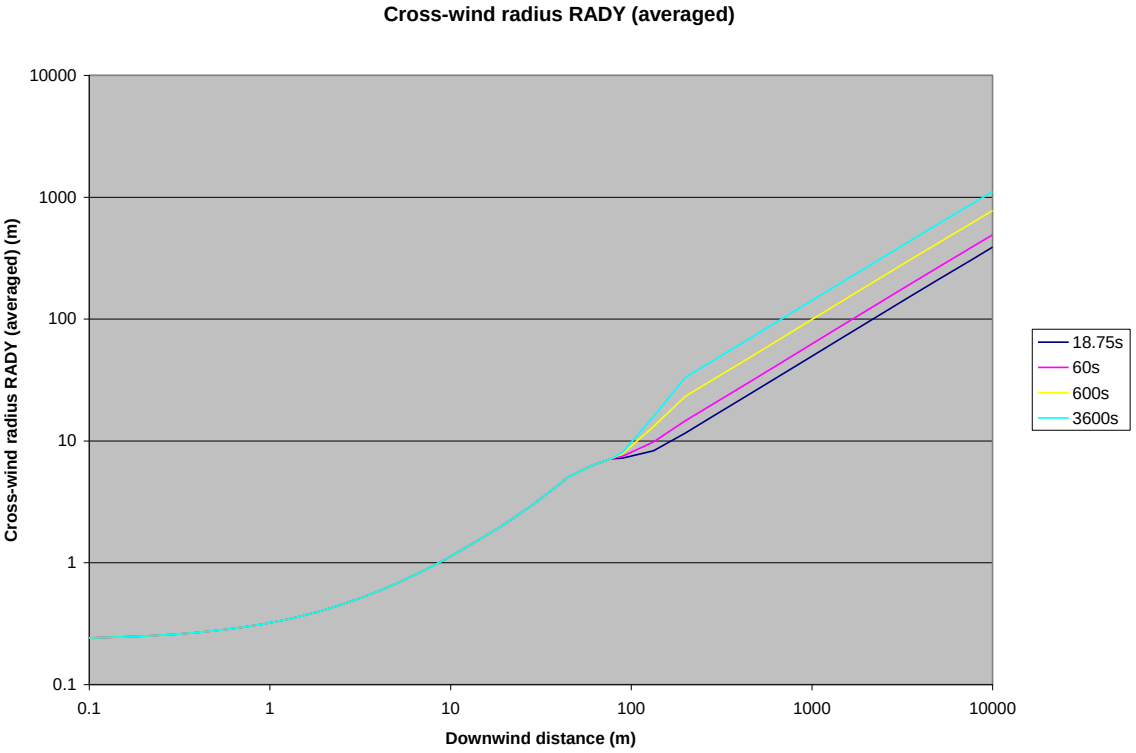

(b) cloud half-width R_y

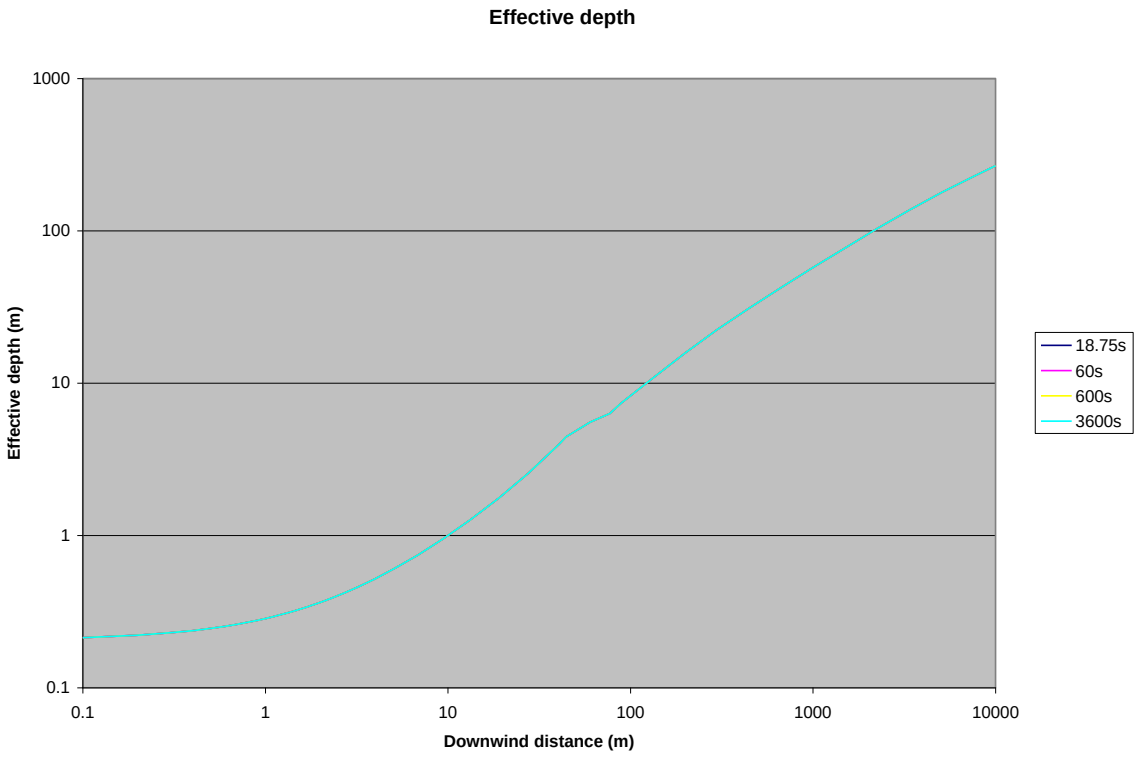

(c) effective cloud depth $H_{eff}(1+h_d)$

Figure 5.22 **Variation of averaging time for touching-down jet base case**
[t_{av}^{core} = 18.75; phase in spread rate; averaging-time method B (old UDM)]
UDM predictions are included for averaging times t_{av} = 18.75, 60, 600, 3600 seconds.

5.2.2 Transition criterion (to update)

Transition parameters

According to the UDM theory manual the UDM passive-transition criterion is expressed in terms of the following transition parameters:

- $r_u = 0.1$, $r_E = 0.3$. These values are in line with HGSYSTEM assumptions[i].
- $r_\rho = 0.015$. This value is in line with the former UDM assumption. Note that CCPS guidelines quotes a range $0.001 < r_\rho = 0.01$. The DEGADIS model adopts 0.001. Since averaging time effects will not be included as long as the transition criterion is not achieved, the larger UDM value is maintained
- $Ri_*^{cr} = 15$. This value assures that $\Phi(Ri_*) < \Phi(Ri_*^{cr}) \approx 2$, and therefore the heavy-gas top-entrainment velocity $u_{top} = \kappa u_*/\Phi(Ri_*)$ at transition is not more than twice as small as its passive limit $u_{top} = \kappa u_*/\Phi(0)$. Again since averaging time effects will not be included as long as the transition criterion is not achieved, a rather large value of the critical Richardson number Ri_*^{cr} is selected.
- $r_{tr} = 2$. This value should be sufficiently large to smoothen the discontinuities between the near-field and far-field passive entrainment and spread-rates.

Sensitivity analysis

To add results of sensitivity analysis to each of the transition parameters for one or more base cases (ground-level heavy, touching down, elevated jet). Compare also sensitivity study carried out by Witlox for HFPLUME/HEGADAS interfacing[i].

Comparison of near-field with far-field passive-entrainment and spread-rates

Values of the Richardson number, entrainment and spread rates are presented in the Table below for a number of test cases. As can be seen the discontinuities at the passive transition point can be quite severe. The choice for the Richardson cut off was originally selected as being $Ri_*^{cr} = 2.35$ [below which $\Phi(Ri_*) = 1$]. In some cases this lead to unrealistic transition distances. Therefore a higher value of Ri_*^{cr} was selected, because zero averaging-time effects apply in the heavy regime and because future implementation of the gravity-collapse criterion may further improve the heavy-gas formulation. The critical Richardson number $Ri_*^{cr} = 15$ was chosen as this would give top-entrainment velocities which would be half those when heavy gas effects die out [$\Phi(Ri_*^{cr}=15) \approx 2$].

Description	Richardson Number at transition	Criterion defining transition	passive far-field / near-field entrainment rate (kg/s m)	passive far-field / near-field spread rate (m/m)
Heavy				
ground-level propane release (non-jet)	1.13	Density	13.1 / 5.9	0.05 / 0.1
ground-level hexane release (non-jet)	1.28	Density	13.2/5.9	0.05/0.13
Elevated jet release of SO_2	16.1 15	Velocity Rich no.	8.4/12.01 9.6/15	0.023/0.46 0.023/0.415[1][2]
Desert Tortoise 1	3.3	Density	51/26.8	0.047/0.13
Maplin Sands 29	3.2	Density	24/9.0	0.05/0.10
Jet				
Jet base case (neutral buoyancy)	0	Velocity	14.4/8.1	0.05/0.03
Touching down jet base case (neutral buoyancy)	0	Velocity	15.3/8.5	0.05/0.04
Ground-level methane release	-5.54	Entrainment	18.2/55	0.024/0.062
Release velocity < wind speed (neutral buoyancy)	0	Velocity	6.2/8.7	0.058/0.1

[1] The explanation for the large differences in the passive and non passive entrainment rates at the transition point is related to the fact that this case was run with 1.5F. This results in low passive spread rates and hence low entrainment rates. The case was run at 5F giving a much smoother transition. Similar results are observed defining this case as a non jet ground-level release.

[2] Transition distance 790 versus 690 m

5.3 Further work

Further work may be as follows:

1. Sensitivity analysis to transition criteria

2. Further improve transition to passive for a range of averaging times (keeping transition zone) and/or implement method removing transition zone. E.g. check AEROPLUME/FARPLUME matching for elevated transition.

3. Investigate further compatibility between near-field and far-field passive dispersion to ensure further consistency, both for elevated dispersion (E_{pas}^{nf} versus E_{pas}^{ff}) and ground-level dispersion (E_{hvy} versus E_{pas}^{ff}).This may be carried out by comparing entrainment rates, spread rates, Richardson numbers, density differences etc. Also check transition criteria adopted for other programs (e.g. AEROPLUME, jet to passive).

SPREADSHEETS

Figure 5.1	Propane_Impact_Windspeed.xls
Figure 5.2	Propane_Impact_Release_Angle.xls
Figure 5.3	Propane_Impact_Release_Velocity.xls
Figure 5.4	Propane_Impact_Instananeous_Windspeed.xls
Figure 5.5	Heavy_B_Spread_Phased.xls – t_{av}^{core} = 600s, r_{tran}^{pass} = 1.01
Figure 5.6	Jet_B_Spread_Phased.xls – t_{av}^{core} = 600s, r_{tran}^{pass} = 1.01
Figure 5.7	TD_Jet_B_Spread_Phased.xls – t_{av}^{core} = 600s, r_{tran}^{pass} = 1.01
Figure 5.8	Heavy_B_Spread_Phased.xls – r_{tran}^{pass} = 1.01
Figure 5.9	Jet_B_Spread_Phased.xls – r_{tran}^{pass} = 1.01
Figure 5.10	Heavy_B_Spread_Phased.xls – r_{tran}^{pass} = 1.01
Figure 5.11	(SMTRN_CORTIM.xls)
Figure 5.12	(SMJTRN_CORTIM.xls)
Figure 5.13	(SMTJTRN_CORTIM.xls)
Figure 5.14	Heavy_A_Spread_Phased.xls – r_{tran}^{pass} = 1.01
Figure 5.15	Jet_A_Spread_Phased.xls – r_{tran}^{pass} = 1.01
Figure 5.16	TD_Jet_A_Spread_Phased.xls – r_{tran}^{pass} = 1.01
Figure 5.17	Heavy_A_Spread_Phased.xls
Figure 5.18	Jet_A_Spread_Phased.xls
Figure 5.19	TD_Jet_A_Spread_Phased.xls
Figure 5.20	Heavy_B_Spread_Phased.xls
Figure 5.21	Jet_B_Spread_Phased.xls
Figure 5.22	TD_Jet_B_Spread_Phased.xls

About DNV

We are the independent expert in risk management and quality assurance. Driven by our purpose, to safeguard life, property and the environment, we empower our customers and their stakeholders with facts and reliable insights so that critical decisions can be made with confidence. As a trusted voice for many of the world's most successful organizations, we use our knowledge to advance safety and performance, set industry benchmarks, and inspire and invent solutions to tackle global transformations.

Digital Solutions

DNV is a world-leading provider of digital solutions and software applications with focus on the energy, maritime and healthcare markets. Our solutions are used worldwide to manage risk and performance for wind turbines, electric grids, pipelines, processing plants, offshore structures, ships, and more. Supported by our domain knowledge and Veracity assurance platform, we enable companies to digitize and manage business critical activities in a sustainable, cost-efficient, safe and secure way.

REFERENCES

[i] Witlox, H.W.M. and McFarlane, K., Interfacing dispersion models in the HGSYSTEM hazard-assessment package, Atmospheric Environment, Vol. 28, No. 18, pp. 2947-2962 (1994)